Shrinkage reducing agent in concrete

The mechanism and its influences on the hydration process and mechanical properties

Jeroen Feij

In partial fulfilment of the requirements for the degree of

Master of Science

In the department of
Materials Science and Engineering
At
Delft University of Technology

Author: Jeroen Feij

Student number: 4417208
Date: 31 March 2020

Master thesis committee:

Chair:	Dr. ir. M.J.M. (Marcel) Hermans	Faculty of 3mE, TU Delft
Committee member:	Dr. G. (Guang) Ye	Faculty of CEG, TU Delft
Committee member:	Dr. I.M. (Ian) Richardson	Faculty of 3mE, TU Delft
Committee member:	Prof.dr.ir E. (Erik) Schlangen	Faculty of CEG, TU Delft
Committee member:	ir. Z. (Zhenming) Li	Faculty of CEG, TU Delft

Acknowledgement

This master thesis was performed to conclude my master Materials Science and Engineering at the Delft University of Technology, with the specialisation Advanced Construction Materials.

I would like to use this opportunity to thank my committee members: Dr. G. (Guang) Ye, Dr. I.M. (Ian) Richardson, Prof.dr.ir E. (Erik) Schlangen, Dr. ir. M.J.M. (Marcel) Hermans and ir. Z. (Zhenming) Li. Their guidance, feedback, and support throughout this research made it possible for me to finalize this master thesis. And I would like to thank Michaël Menting for his guidance and for the opportunity to perform my research at ABT B.V. and Maiko van Leeuwen for his support with the experiments and the great conversations.

Lastly, a massive thank you to my family for all the support during my entire college career and especially over the last year. I am proud of you and I would not have been able to achieve this without you all.

Zoetermeer, May 2020

Jeroen Feij

Abstract

In the Netherlands large monolithic floors are commonly built without dilation joints. In floors without dilation joints, cracks can form due to drying shrinkage. Currently, shrinkage strains in undilated floors are controlled by applying large amounts of reinforcements and reducing the thickness of the floors. However, drying shrinkage induced cracking sometimes still occurs. A solution for reducing the drying shrinkage strains and improving the concrete durability is applying shrinkage reducing agents (SRAs).

Due to climate change summers become increasingly warmer. Furthermore, CO_2 emission of cement production are increasing annually and should be reduced (Grădinaru, 2017; Andrew, 2018). With current in-situ concrete casting methods, the days with acceptable casting conditions are reducing. Shrinkage reducing agents have the potential to allow casting under harsh conditions and to reduce drying shrinkage (Sant, 2012). The reduction in drying shrinkage will result in lower possibility of drying shrinkage cracking, increasing the durability of the concrete. By applying an SRA and with good mix design, drying shrinkage reductions up to 40% can be achieved. However, information about the mechanism of drying shrinkage reduction by SRAs is limited (Zuo et al., 2017; Zhan & He, 2019).

To research the mechanism and the degree of shrinkage reduction of a shrinkage reducing agent, a series of tests were performed. One specific shrinkage reducing agent was investigated, Sika Control 40. The mechanism of shrinkage reduction and its side effects were investigated. Both cement paste and concrete samples were prepared with different SRA content. A reference mixture without SRA and three mixtures with SRA contents of 0.52w%, 1.56w% and 2.61w% of cement were used. These SRA concentrations are based on the minimum, 0.52w%, to maximum, 2.61w%, prescribed concentrations. An intermediate value of 1.56w% was used to further investigate the influence of SRA concentrations.

The mechanism of shrinkage reduction for agents like Sika Control 40, are based on lowering the surface tension of the pore liquid of concrete. According to the Laplace law (see Equation 1) on capillary pressure

$$\Delta p = \frac{2\gamma \cos\theta}{r}, \qquad \text{Equation: 1}$$

surface tension is proportional to the capillary tensile forces which cause drying shrinkage to occur. Lower surface tension can result in less drying shrinkage. Sika Control 40 is a surfactant therefore, the molecules have a hydrophilic and a hydrophobic group (Rosen, 2004). When Sika Control 40 is added to the concrete mix the molecules will position themselves on the solid-liquid interface because of these molecular groups and thus lowering the surface tension (Rosen, 2004). The layer of surfactant molecules forms a barrier between the water and the unhydrated cement. However, this layer of surfactant molecules can negatively influence the hydration rates and consequently the mechanical properties. To investigate the mechanism of drying shrinkage reduction and the influence of the SRA on the hydration process, tests were performed on the rate of hydration, surface tension, porosity, cement paste shrinkage and cement paste strength. It is found that higher concentrations of SRA resulted in lower surface tension, lower rate of hydration, higher porosity, and a decrease in both compressive as flexural strength of cement paste.

The influences on the mechanical properties, in other words, compressive strength, shrinkage and elastic modulus of concrete samples were also determined. The concrete mix had a cement content of 350 kg/m^3 with a water cement ratio of 0.48. SRA dosages of 0.52 w%, 1.56 w% and 2.61 w% of cement were used. It was found that higher concentrations of SRA resulted in a decrease of drying shrinkage of 36-48% after 28 days of hydration. Compressive strength decreased with increasing SRA content, while the elastic modulus remained similar.

Overall, the experimental results showed that applying Sika Control 40 is an effective method for reducing drying shrinkage when concentrations of 1.56 w% and 2.61 w% are used. The SRA actively lowers the surface tension of the pore liquid. Due to the hydrophilic and hydrophobic molecular groups the SRA positions itself on the solid-liquid interface in the pores of hardened cement paste. The capillary tensile force induced by the surface tension of capillary water is reduced resulting in lower drying shrinkage. However, for increasing SRA concentrations the rate of hydration was lower, as well as the total heat of hydration. The shrinkage reducing agent forms a barrier between the unhydrated cement particles and the water and dissolution of alkalis is slower (Rajabipour et al., 2008), slowing down the hydration process. The overall porosity of the cement paste increased and especially the volume of gel pores <1µm increased for higher SRA dosages. This resulted in lower flexural and compressive strength for cement paste and concrete samples. An SRA concentration of 2.61 w% resulted in slightly higher drying shrinkage reduction with respect to 1.56 w%, while the decrease in rate of hydration and strength were very similar. In practice the extra reduction in drying shrinkage for an SRA concentration of 2.61 w% should be weighed versus the costs and slight decrease in mechanical properties.

Table of contents

1) Introduction

In construction, concrete is a very commonly used material for monolithic floors. Concrete is most widely used due to its low cost and good durability if applied correctly. ABT B.V. makes these monolithic floors, for example, in large warehouses. In the past most large slabs were dilated but, since the last two decades it is common in the Netherlands that industrial floors are made without dilation joints. Without dilation joints, monolithic floors are more prone to cracking, because the concrete is restrained to shrink or expand (Weiss & Shah, 2002). Shrinkage strains in these undilated floor slabs are currently controlled with a large amount of reinforcement and by using a thinner structural thickness. Shrinkage reducing agents (SRAs) are additives that can reduce shrinkage strains in concrete and thus reduce the tendency of drying shrinkage cracking (Collepardi et al., 2005). When applied correctly, quality of these thinner undilated floor slabs can be improved and up to 50% of the raw materials can be saved compared to dilated structures.

The use of monolithic undilated slabs can also be applied in basement raft foundation slabs. More recently, large underwater concrete slabs are cast using similar techniques. These structures are designed within the small bandwidth of good execution, a good quality construction, high amount of reinforcement and a good concrete mix design. Hereby, the shrinkage strains are controlled. Due to climate change summers become increasingly warmer. Furthermore, CO_2 emission from cement production are increasing annually and should be reduced (Grădinaru, 2017; Andrew, 2018). With current in-situ concrete casting methods, the days with acceptable casting conditions are reducing. Shrinkage reducing agents have the potential to allow casting under harsh conditions, to reduce drying shrinkage (Sant, 2012) and to design undilated structures to reduce the amount of used materials. The reduction in drying shrinkage will result in less drying shrinkage cracking, increasing the durability of the concrete.

The environment where the concrete is applied has an influence on the hardening behaviour and the material properties of concrete during its life cycle. This is especially the case when shrinkage of concrete is considered. The cement in the concrete mix undergoes a chemical shrinkage of approximately 6.25 cm^3 per 100 grams of cement. Besides the chemical shrinkage concrete can undergo autogenous, drying, and plastic shrinkage and shrinkage due to change in temperature and carbonation. Shrinkage of concrete, when restrained, will induce tensile stresses. When these stresses exceed the concrete strength, concrete cracking might occur. These cracks can reduce durability and strength resulting in reduced performance. The repair of cracks in concrete can be time consuming and costly. Cracks can be injected or filled with various materials like PUR (Polyurethane). The period needed for hardening of these injected materials can result in downtime for production lines or temporary unavailable areas. Hence, looking at possibilities to reduce shrinkage is desirable.

A good mix design of the concrete and appropriate curing after casting reduces the amount of plastic shrinkage and autogenous shrinkage of concrete (Neville, 1995). Chemical shrinkage always occurs because of the nature of the chemical reaction. The hydrated cement occupies a lower volume than the reactants including the unhydrated cement and water. Drying shrinkage can also be reduced by a good mix design and by applying shrinkage reducing admixtures. By applying an SRA and with good mix design, drying shrinkage reductions up to 40% can be achieved (Collepardi et al., 2005). A large variety of shrinkage reducing agents are commercially available which work in different manners. These agents can improve the behaviour of fresh concrete and the properties of hardened concrete. Examples are improved workability and less shrinkage. These shrinkage reducing agents work, but scientific information on the mechanism of shrinkage reduction and effects on the hardening and

material properties of concrete is limited (Collepardi et al., 2005; Maltese et al. 2005; Zuo et al., 2017). In this master thesis, the mechanism of one specific shrinkage reducer, Sika Control 40, and effects on the hydration process and material properties of concrete are investigated.

To obtain a better insight into the mechanism of shrinkage reduction of Sika Control 40, and the effects this SRA has on the hydration process and material properties of hardened concrete, the following research question was formulated:

'***What is the mechanism of shrinkage reduction for shrinkage reducing agent Sika Control 40 and what are the influences on the hydration process and development of material properties?***'

Besides the scientific value of this research, this master thesis is based on the curiosity concerning practical implications of the SRA Sika Control 40. The interest lies especially with this SRA, because ABT, the company for which this research is performed, is interested in its possibilities. Multiple series of experiments have been performed and a literature study on the different behaviours and mechanisms of shrinkage reducers was undertaken. This research will give better insight in the mechanism of Sika Control 40 and its effect on the concrete properties.

In chapter 2 the theoretical background of types of shrinkage of concrete and shrinkage reducing agents is summarised. In addition, the theory and mechanism of SRAs is discussed. In chapter 3 an overview of test setups and methodology is given on the influences of applying SRA in cement paste and concrete. An analysis of respective results is presented in chapter 4. Thereafter, in chapter 5 the results are combined to discuss and explore the connections between the individual test results. Scientific and practical implications of this research and the conclusion are given in chapter 6.

2) Theoretical background

In the concrete research field extensive research has already been performed on shrinkage mechanisms (Zhan & He, 2019). Steps are taken and still being made to research different methods of reducing shrinkage. A theoretical background is given on the phenomena of different types of concrete shrinkage. A more elaborate view is given on the mechanism of drying shrinkage and the current reduction methods for drying shrinkage. The focus is placed on drying shrinkage as reducing this type of shrinkage is the most useful solution for the practical problem of constructing monolithic floor slabs without dilation joints.

The scope of this research is on the mechanisms and influences of shrinkage reducing agents (SRAs). Therefore, this type of shrinkage reduction method is discussed more elaborate by reviewing the topics of surface tension, surfactants, the SRA Sika Control 40, and the discourse of the downsides of applying SRAs. Lastly, the scientific objectives of this research are set.

2.1) Types of shrinkage

From the moment of mixing of the concrete until decades after initial hardening, concrete undergoes shrinkage. In different stages of concrete hardening various types of shrinkage occur. A division is made between thermal shrinkage, plastic shrinkage, chemical shrinkage, autogenous shrinkage, drying shrinkage, and carbonation shrinkage. A summary of when these types of shrinkage play a significant role is given in the table below (Table 2.1). In addition, the mechanism of each type of shrinkage is briefly discussed.

Table 2.1 Types of shrinkage and their respective effects

Type	Period of effect	Effect
Thermal shrinkage	Always present	Thermal expansion or shrinkage due to temperature change.
Plastic shrinkage	Hours-Days	Risk of large cracks due to excessive evaporation of water at concrete surface.
Chemical shrinkage	Days-Weeks	Internal volume reduction due to ongoing hydration; No length reduction on macroscale.
Autogenous shrinkage	Days-Weeks	Risk of cracking due to capillary tension caused by ongoing hydration; Barely any length reduction on macroscale.
Drying shrinkage	Days-Years	Risk of cracking due to capillary tension caused by evaporation of pore water; Severe length reduction on macroscale.
Carbonation shrinkage	Years-Decades	Crackle-shaped cracks on concrete surface; No length change on macroscale.

2.1.1 Thermal shrinkage

Thermal shrinkage and expansion are a variation in volume due to temperature changes. When temperature increases concrete expands, and concrete shrinks when it cools down. The extent of

volume change depends on the thermal expansion coefficient of the concrete and the change in temperature.

During cement hydration, heat is generated and the concrete increases in temperature. This heat dissipates over time and the concrete cools down. In thin concrete members this process is rather equal throughout the cross section of the member (Neville, 1998; Reinhardt, 1995). In thick and large volume members, thick floors for example, the surface will cool down more rapid than the centre of the member. This results in a temperature gradient. Because the surface is colder it is contracting due to thermal contraction, the centre is still warm and expanded due to thermal expansion. Resulting in tensile stresses in the concrete. When this tensile stress exceeds the concrete tensile stress, cracks will form.

Thermal shrinkage is most often a problem during the first days of hydration but, can also occur when a concrete surface is exposed to extreme temperatures. Thermal shrinkage cracking can be limited by limiting the thermal temperature differential, normally 20°C. Good mix design and choice of cement type with lower heat of hydration can reduce thermal shrinkage.

2.1.2 Plastic shrinkage

Plastic shrinkage cracks occur when excessive amounts of water evaporate at the concrete surface during hardening (Neville, 1995; Reinhardt, 1998). When freshly mixed concrete is cast, mixing water will start to bleed to the surface. This bleeding water will evaporate from the surface if no precautions are made. Large horizontal surfaces exposed to wind, direct sunlight and low relative humidity can accelerate the evaporation (Neville, 1995; Reinhardt, 1998). When the water at the surface evaporates faster than it can be replaced by bleeding water, tensile stresses will develop in the concrete because pores desiccate. The fresh concrete does not have the capacity to resist these tensile stresses so cracks will form. Appropriate moist curing after casting and preventing evaporation at the concrete surface can prevent plastic shrinkage cracking.

2.1.3 Chemical shrinkage

During the hydration process of cement, a decrease in volume of the system can be observed. The total volume of the hydration products is smaller than its unhydrated cement and mixing water. This phenomenon is called chemical shrinkage (Zhang et al., 2013). Chemical shrinkage starts as soon as the hydration process starts. When the concrete is still plastic, chemical shrinkage can be measured externally because the concrete cannot resist any volume changes. After setting, chemical shrinkage is no longer observed as external volume change, the concrete rather reduces in volume by creating air voids inside the concrete.

2.1.4 Autogenous shrinkage

Autogenous shrinkage occurs after setting in young concrete especially in concrete mixes with low water to cement ratios (Lura, 2003). During the hydration process the available water is rapidly used to form hydration products. Especially at water to cement ratios lower than 0.42 ongoing hydration results in empty pores. The surface tension of water and the shape of the water meniscus inside these pores, induce a tensile stress on the surrounding concrete. This tensile stress causes the concrete to shrink or even crack when it exceeds the concrete tensile strength.

Autogenous shrinkage can be reduced by wet curing after casting, internal curing with super absorbent polymers (Craeye, Geirnaert & De Schutter, 2011) or saturated porous aggregates. These methods provide water to avoid self-desiccation.

2.1.5 Carbonation shrinkage

Carbon dioxide in the atmosphere can react with the hydrated cement in the presence of water. This reaction converts calcium hydroxide crystals into calcium carbonate (Neville, 1995). The volume of calcium carbonate is smaller than that of calcium hydroxide. Therefore, this reaction results in carbonation shrinkage. Carbonation shrinkage is limited to the surface layer which is exposed to the air. The ingress of carbon dioxide is very slow, and the magnitude of shrinkage is very low compared to long term drying shrinkage. Because carbonation shrinkage is limited to a thin surface layer and because of its low shrinkage it is of low significance. However, a second problem of carbonation of concrete is that the alkalinity lowers, because calcium hydroxide crystals are converted into calcium carbonate. This becomes a problem when the carbonation depth reaches the reinforcement steel and corrosion of the reinforcement can start. Dense concrete and appropriate concrete reinforcement cover depth is a good solution to avert this problem.

2.1.6 Drying shrinkage

The last type of shrinkage discussed is drying shrinkage. As mentioned, this phenomenon is more elaborately discussed as in concrete structures without dilation joints the main cause for cracking is drying shrinkage. Due to the drying shrinkage, tensile stresses are induced and if these tensile stresses exceed the concrete strength, cracks can form (Neville, 1995; Reinhardt, 1998; Eberhardt, 2011). First, the phenomenon of drying shrinkage is explained more in-depth. In addition, the closely related phenomena of creep and relaxation are discussed before getting insight in the methods of reducing drying shrinkage.

2.1.6.1 The phenomenon of drying shrinkage

Drying shrinkage occurs when water from the pores evaporate due to change in relative humidity. The rate at which water evaporates is dependent on the environment as with the case of plastic shrinkage. Temperature, relative humidity, wind velocity, pore structure and geometry all influence the rate of evaporation. The pore structure is strongly related to the water to cement ratio, cement type and degree of hydration (Neville, 1995). In larger pores the evaporation of water is easier and therefore, larger pores will empty first, and the water will remain in the smaller pores. Smaller pores result in higher capillary tension because the water pulls harder on the matrix around the pore. This can be described with the Laplace law (Lura, 2003, p. 173):

$$\Delta p = \frac{2\gamma \cos\theta}{r}, \qquad \text{Equation: 2}$$

where γ_w is the surface tension of the capillary water, θ is the contact angle on the solid-liquid interface and r is capillary pore diameter. So, in smaller pores the capillary tension is higher that is why the water climbs higher in small tubes as depicted below.

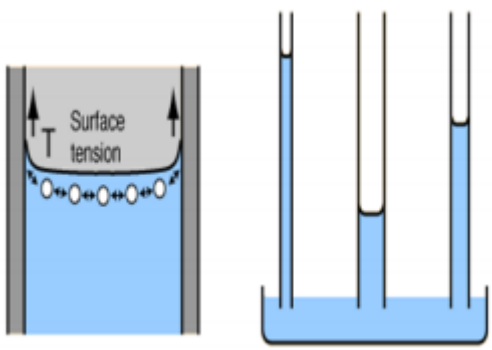

Figure 2.1 Capillary tension in tubes with different diameter (Ben Mya, 2020)

When pores are emptied due to evaporation of water, the surface tension of water causes a water meniscus to form (Neville, 1995; Reinhardt, 1998; Eberhardt, 2011). Due to the surface tension and the shape of the meniscus capillary tensile stresses are exerted on the concrete around the pore. This tensile force causes the concrete to shrink. If the capillary tensile stress is higher than the concrete tensile strength, cracks will form in the concrete. The amount of shrinkage and possible cracking depends on the mechanical properties of the cement paste and the aggregates. Aggregates with high stiffness result in lower concrete drying shrinkage (Reinhardt, 1998).

As mentioned, drying shrinkage depends on the relative humidity and the water meniscus formed due to the surface tension of water. The relative humidity in a circular pore can be calculated with the Kelvin equation (Lura, 2003; Jensen & Bentz, 2002):

$$RH = \exp\left(-\frac{2\gamma * V_m * cos\theta}{r * R * T}\right), \qquad \text{Equation: 3}$$

where:

RH = Relative humidity

γ = Surface tension of water [N/m]

V_w = Molar volume [m^3/mol]

θ = Angle of contact between liquid and solid

r = Pore radius

R = Gas constant for ideal gas [J/(mol*K)]

T = Absolute temperature [K]

When the Laplace law and Kelvin equation are combined, it can be observed that the capillary stress increases when the relative humidity decreases and vice versa. Therefore, when the relative humidity is lower than 40% then deformation in the concrete matrix is controlled by the change in surface tension of the gel particles in the adsorption layer (Reinhardt, 1998; Lura, 2003). The surface tension of the gel particles decreases, and the cement paste shrinks due to the evaporation of the absorbed water. However, when the relative humidity is between 40-80%, the disjoining pressure is the driving mechanism for shrinkage (Reinhardt, 1998; Lura, 2003). Disjoining pressure is active in areas where the distance between solid surfaces are smaller than two times the thickness of the free adsorbed water (Lura, 2003). When water evaporates this layer of water between solid particles decreases in width. Causing the solid particles to move closer together, resulting in shrinkage of the cement matrix (see Figure 2.2).

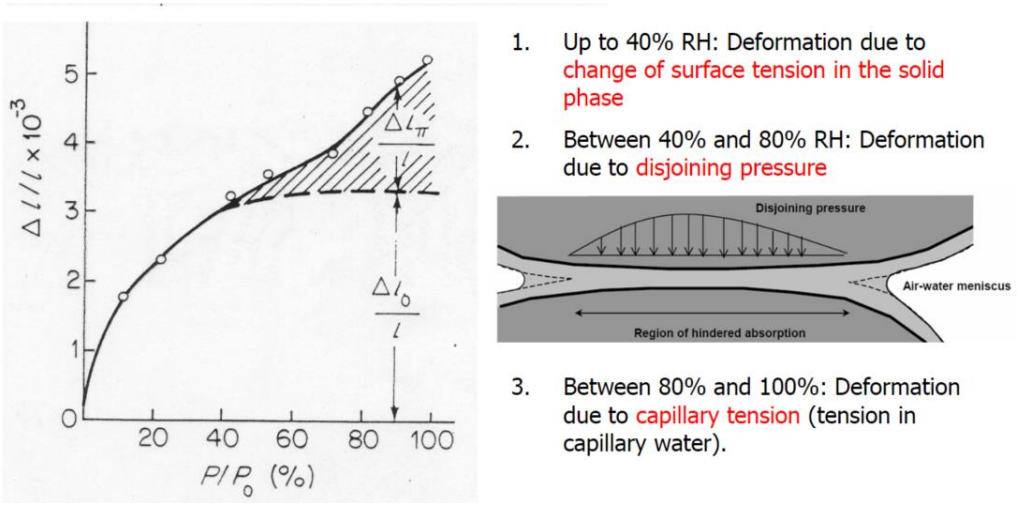

Figure 2.2 Shrinkage mechanisms. Copied from (Reinhardt, 1998, p. 151; Lura, 2003, p. 17)

2.1.6.2 Shrinkage cracking

Shrinkage cracking of hardened cement paste and concrete is not solely based on the amount of shrinkage. Creep and relaxation are two phenomena that can influence cracking in concrete alongside shrinkage. The amount of relaxation and creep that occurs is strongly dependant on the material properties and applied stress (Neville, 1995). Creep under tension negatively influences the amount of strain and can increase risk of cracking. Relaxation positively reduces the stress in the concrete and therefore reduce the risk of cracking. The phenomena of creep and relaxation are briefly touched upon.

Creep

Creep is the increasing deformation over time under a constant load (Reinhardt, 1998; Li, 2001). Creep causes steady increments of strain under a constant load. This can be a problem when creep is not considered during construction. Due to creep, pre-tensioned concrete might shorten over time and subsequently increase the load on the reinforcements. The pre-tensioning steel should be adequately strong to counter this.

Whenever a specimen is drying while under load it is usually assumed that creep and shrinkage are additive. This is illustrated in Figure 2.3. Creep (2) is calculated as the difference between time dependant deformation and the shrinkage, (1), of an unloaded sample stored under similar conditions. However, creep and shrinkage are interdependent. Shrinkage increases the amount creep in a sample, so this conception is not correct. Because shrinkage increases creep, a division is made between basic creep and drying creep. In practice creep and shrinkage occur simultaneously and structures are often exposed to evaporation of water, therefore the simplification that

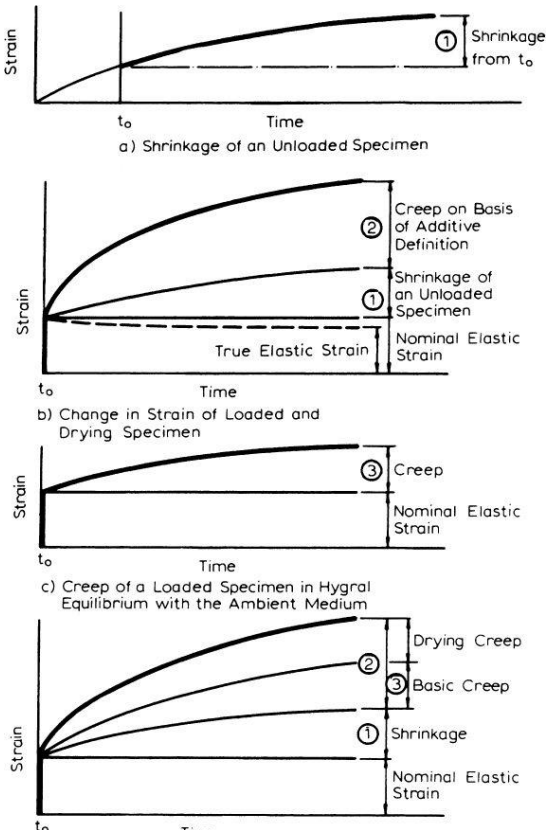

Figure 2.3 Time-dependent deformations in concrete subjected to a sustained load (Neville, 1995)

creep and shrinkage are additive is effective (Neville, 1998).

Relaxation

Relaxation is the decrease of load under constant deformation (Reinhardt, 1998). With respect to shrinkage strains, relaxation is a pleasant phenomenon. Due to relaxation, shrinkage tensile stresses will decrease over time under constant shrinkage deformation. Relaxations lowers the risk of shrinkage cracking because the tensile stress reduces over time.

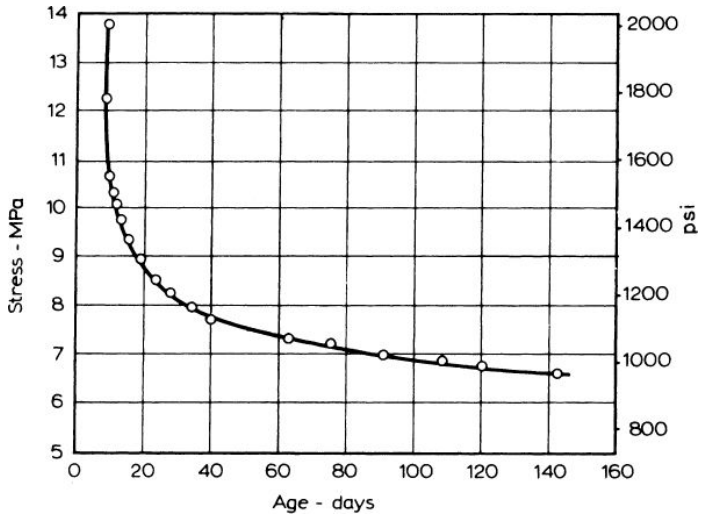

Figure 2.4 Relaxation of stress under a constant strain of 360x10^{-6} (Neville, 1995)

Shrinkage and creep induce tensile stresses, relaxation reduces these stresses. When the induced tensile stresses exceed the tensile strength of concrete cracks can occur. This is schematically shown in Figure 2.5.

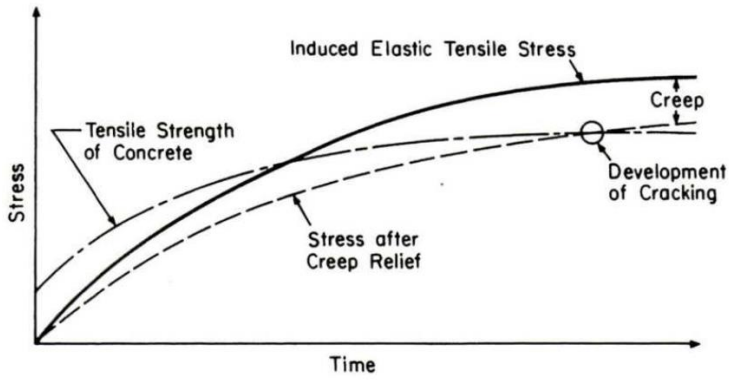

Figure 2.5 Schematic overview of crack development and interaction between shrinkage stress and creep (Neville, 1995)

By reducing the shrinkage strains with shrinkage reducing agents the tensile strength of concrete is less likely to be exceeded. Applying SRAs will positively reduce the induced capillary tensile stress which causes concrete to shrink and possibly crack. However, the influence of SRA on creep and relaxation was not investigated in this research. Therefore, based on this research, no conclusion can be drawn on the influence of SRAs on the formation of cracks.

2.2) Reducing drying shrinkage

Drying shrinkage is a phenomenon that occurs due to interactions between surface tension, relative humidity, and pore size among other things. Methods for reducing drying shrinkage mainly focus on limiting desiccation of the pores and on reducing the surface tension of water (Zhan & He, 2019; Lura,

2003; Zuo et al., 2019). The main methods are using internal curing, proper curing after concrete casting, using shrinkage compensating agents and shrinkage reducing admixtures (SRAs).

2.2.1 Internal curing

A lot of research has been performed on the method of internal curing, especially for reducing autogenous shrinkage (Lura, 2003). Internal curing reduces the capillary tension by adding saturated polymers or porous aggregates. The water that can be extracted from the polymers or porous aggregates fill emptied pores, lowering the capillary tension. Resulting in less autogenous shrinkage and less drying shrinkage.

2.2.2 Curing

Curing of concrete after casting ensures that the surface exposed to the air remains wet. This is specifically important to reduce plastic shrinkage (Neville, 1995). It also adds extra water in the pores of the concrete reducing drying shrinkage during the first days. This allows the concrete to increase strength to counter capillary forces after curing is stopped. Drying shrinkage cracking will be reduced although drying shrinkage will merely be delayed.

2.2.3 Shrinkage compensating agents

Shrinkage compensating agents can be expansive cements that form ettringite or calcium hydroxide during hydration (Nagataki, 1998; Szilagyi, 2007; Winnefeld, 2010). Ettringite and calcium hydroxide have a larger volume than their unhydrated components. This will result in expansion of the cement paste countering a part of the drying shrinkage (Mather, 1970). The timing of these expansive agents is unreliable, currently no consistent method in controlling the expansion exists (Collepardi, 2005). Normally the expansion takes place during cement hydration, however, drying shrinkage only starts after days to weeks. Therefore, the expansion can be completed before drying shrinkage starts.

2.2.4 Shrinkage reducing agents

The last discussed method for reducing drying shrinkage is by using shrinkage reducing agents (SRAs). Above mentioned methods are already researched extensively (Jensen & Lura, 2006) or are found unreliable (Carballosa et al., 2015), therefore a particular interest is taken in the SRAs. In addition, SRAs seem to be effective in lowering capillary stresses because they actively reduce the surface tension of water.

Firstly, a theoretical background is given in the general working of SRAs with an explanation of the phenomenon of surface tension. Secondly, the mechanism and behaviour of surfactants is discussed as SRAs are a type of surfactant. Subsequently, the characterisation of SRA Sika Control 40 is discussed. Lastly, downsides of applying SRAs and unknown effects of SRAs are discussed.

2.2.4.1 Mechanism of shrinkage reducing agents

Shrinkage reducing agents (SRAs) are a type of surfactant. It is a chemical with a hydrophilic and a hydrophobic part that can lower the surface tension. Lowering the surface tension results in lower capillary tension and therefore, less drying shrinkage. The surfactant locates itself on the solid-liquid interface oriented with the hydrophilic part towards the liquid, water, and the hydrophobic part towards the solid, concrete (Rosen, 2004). This occurs because the total free energy of the solution will be lowered, and this is energetically more favourable. From previous research it is known that SRAs can reduce drying shrinkage (Collepardi et al., 2005; Zhan & He, 2019; Zuo et al., 2019).

Surface tension

Surface tension is the tendency to reduce the surface area and find the lowest energy state. Water has a surface tension of 72.75 mN/m at 20 °C (Rosen, 2004).

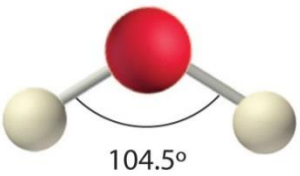

Figure 2.6 H_2O molecule (Chemistry Libretexts, 2019)

The hydrogen atoms and oxygen atom in a water molecule are not in line with each other, there is an angle of 104.45 degrees between the two hydrogen atoms. Therefore, the polar centres of the H_2O molecule do not coincide. Thus, the H_2O molecule is polar with an electrical dipole moment.

The polarity of water makes it possible for the H_2O molecule to form hydrogen bonds. One molecule can form up to four hydrogen bonds with neighbour molecules. These hydrogen bonds are the cause of a high surface tension in water (Rosen, 2004). Due to hydrogen bonding there is a large cohesive force between H_2O molecules. At the interface of water with, for example air, this cohesive force between water molecules is stronger than the interactive force of water with air. At the surface there are less possibilities of hydrogen bonds because the water molecule is not surrounded by neighbouring water molecules. The water molecule at the interface are not interacting on all sides equally. This is the explanation for the bulge that can exist in the water surface.

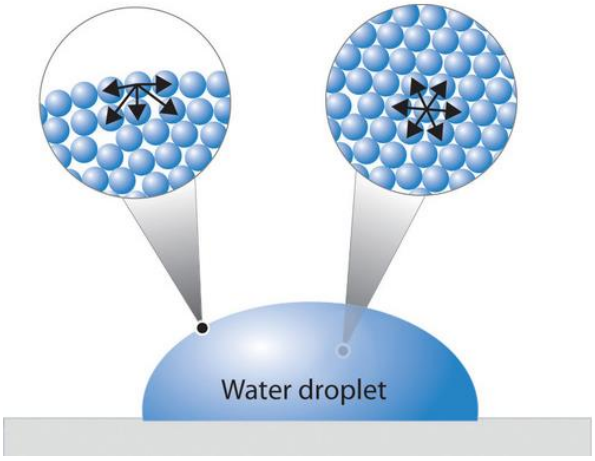

Figure 2.7 Surface tension of water, less interactions at the surface. (Chemistry Libretext, 2019.)

2.2.4.2 Surfactants

As most of the SRAs are surfactants, an overview is given here on the diverse mechanisms behind surfactants. Surfactants can be detergents, foaming agents, wetting agents, emulsifier, and dispersants. These different surfactant types have different chemical compositions. Based on this chemical composition these surfactants react differently. This is due to different hydrophobic and hydrophilic groups these surfactants have (Rosen, 2004). To obtain more insight a brief introduction is given on the hydrophobic and hydrophilic groups of surfactants.

Hydrophobic part of a surfactant molecule

An overview of the different hydrophobic groups is shown in Figure 2.8, and as an example influences of the length of the hydrophobic group and the amount of branching are explained.

1. Straight-chain, long alkyl groups (C_8–C_{20})
2. Branched-chain, long alkyl groups (C_8–C_{20})
3. Long-chain (C_8–C_{15}) alkylbenzene residues
4. Alkylnaphthalene residues (C_3 and greater-length alkyl groups)
5. Rosin derivatives
6. High-molecular-weight propylene oxide polymers (polyoxypropylene glycol derivatives)
7. Long-chain perfluoroalkyl groups
8. Polysiloxane groups
9. Lignin derivatives

Figure 2.8 Hydrophobic groups (Rosen, 2004)

Influence of length of hydrophobic group: The length of a hydrophobic group impacts solubility of the surfactant (Rosen, 2004). Longer chains mean that a surfactant has lower solubility in organic solvents, closer packing at the interface, increased tendency to form micelles, increased melting point and increased sensitivity. Most favourable for the use of surfactants is a short hydrophobic group. This results in a better solubility and less micelle formation. Micelles are groups of surfactant molecules that aggregate in the bulk of the liquid. Micelles will form at a specific critical micelle concentration (CMC), dependant on the length of the hydrophobic group. Longer groups lower the critical micelle concentration meaning that less surfactant can be effectively added to the water (Rosen, 2004). Surfactants are most effective when located on the solid-liquid interface, therefore micelle formation is unfavourable. Thus, short hydrophobic groups are most effective.

Influence of branching and unsaturation: Branching and unsaturation of the hydrophobic group has interesting influences on the behaviour of the surfactant. When the group is more branched it increases solubility, decreases melting point of the surfactant, and causes looser packing of the surfactant at the interface. Similar to the length of the hydrophobic group, branching decreases the critical micelle concentration (Rosen, 2004). The balance of solubility, critical micelle concentration and preferred applicable concentrations can be used to select an effective hydrophobic group.

Hydrophilic part of surfactant molecule

The hydrophilic part can be anodic, cathodic, non-ionic and zwitterionic (Rosen, 2004). Anodic surfactants have a negative charge at the surface-active part, for example RCOO-Na+. Cationic surfactants bear a positive charge at the surface-active part, RNH_3+Cl-. Non-ionic surfactants bear no charge at the surface-active part. Zwitterionic surfactants bear both positive and negative charges. These four different types interact in different ways with the cement and the capillary pore water. Which also lowers the surface tension by different amounts. For example, hydrocarbon surfactants can reduce the surface tension down to about 30mN/m and fluorocarbon surfactants to about 20mN/m. The large variety in surfactant composition and their characteristics mean that surfactants can have widespread and specific uses. In this research the surfactant Sika Control 40 is used in concrete which has a harsh alkaline environment. Next the composition and behaviour of Sika Control 40 are investigated.

2.2.4.3 Sika Control 40

As this research is based on the Sika Control 40 admixture, its composition and functionality are investigated. Sika control 40 consists of neopentyl glycol, this is a double alcohol molecule. This makes it a non-ionic surfactant. Rosen (2004) states the advantages and disadvantages of polyolefin

elastomers straight chain alcohols (alcohol ethoxylates, AEs) which is like neopentyl glycol in behaviour. In addition, AEs are more tolerant of high ionic strength and hard water and they are more stable in hot alkaline solutions. These characteristics are especially beneficial when applied in cement. Cement has a lot of ionic bonding and the pore solution contains a lot of calcium carbonate, so it is 'hard water'. During hydration, the concrete heats up resulting in a hot alkaline environment where this surfactant has an optimal performance. One of the disadvantages is that in high concentrations AEs tends to bleed from powders giving poor powder properties. Since, Sika control 40 is applied in liquid form, this will not be a problem.

To research the behaviour and mechanics of Sika Control 40, the bonding behaviour is investigated. As stated previously the different surfactant types will work in different ways (Rosen, 2004). Anionic and cathodic surfactants will use ion exchange and ion-pairing at the water-concrete interface. Ion exchange involves the replacement of counter ions absorbed onto the solid substrate by similarly charged surfactant ions, so this is dependent on diffusion rate. Ion pairing is the adsorption of surfactant ions from solution onto oppositely charged sites unoccupied by counter ions. Non-ionic surfactants like the Sika control 40 work via hydrogen bonding or via Lewis acid-Lewis base reaction. These mechanisms are shown below.

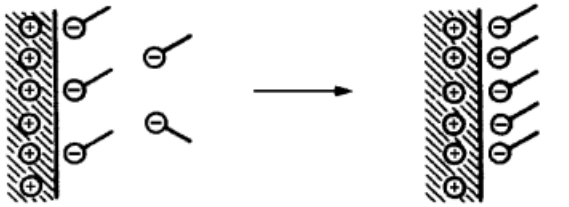

Figure 2.9 Ion pairing (Rosen, 2004)

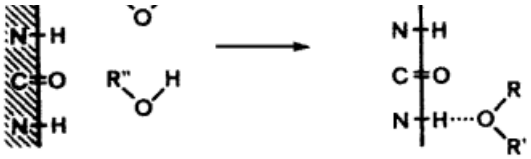

Figure 2.10 Hydrogen bonding (Rosen, 2004)

Due to its molecular structure, Sika Control 40 molecules take the place of the water molecules at the interface between the water and concrete by forming hydrogen bonds with cement particles. The surface tension of the water is lowered and so is the contact angle of water with cement. Therefore, according to the Laplace law in equation 1:

$$\Delta p = \frac{2\gamma_w \cos\theta}{r},$$

the capillary forces will be lowered resulting in lower capillary tensile stresses and ultimately in less drying shrinkage.

In Figure 2.11 the shrinkage reduction in one SRA modified mortars dependant on dosage and time is shown (Eberhardt, 2010). Table 2.2 shows the exact values. It can be observed that the SRA reduces drying shrinkage. The major part of shrinkage reduction is gained in the first 50 days well before drying

equilibrium is reached. After approximately 30 days of drying the absolute increase in shrinkage proceeds independently of the SRA dosage (Eberhardt, 2010).

Table 2.2 Free drying shrinkage of SRA mixes with different concentrations as a function of time (Eberhardt, 2010)

time	shrinkage reduction [%]		
14d	37	44	57
28d	17	26	39
70d	16	20	32
180d	12	14	28
364d	10	14	24
SRA*	1.5%	2.5%	5.0%

*wt.-% of mixing water

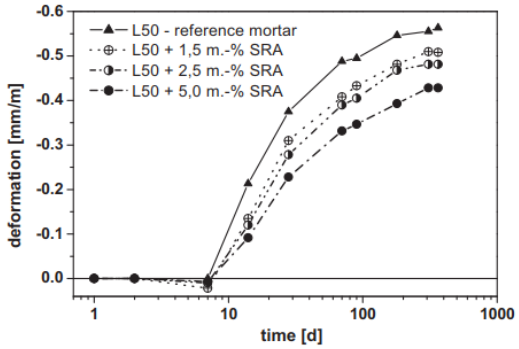

Figure 2.11 Free drying shrinkage of SRA mixes with different concentrations as a function of time (Eberhardt, 2010)

Collepardi et al. (2005) researched the amount of shrinkage reduction of concrete with an SRA similar to Sika control 40. In concrete with a w/c ratio of 0.40, 390 kg/m^3 cement content and one week of wet curing it can be observed in Figure 2.12 that the shrinkage reduction is approximately 35-40% when the concrete is exposed to 25 degrees Celsius air temperature and 60% relative humidity.

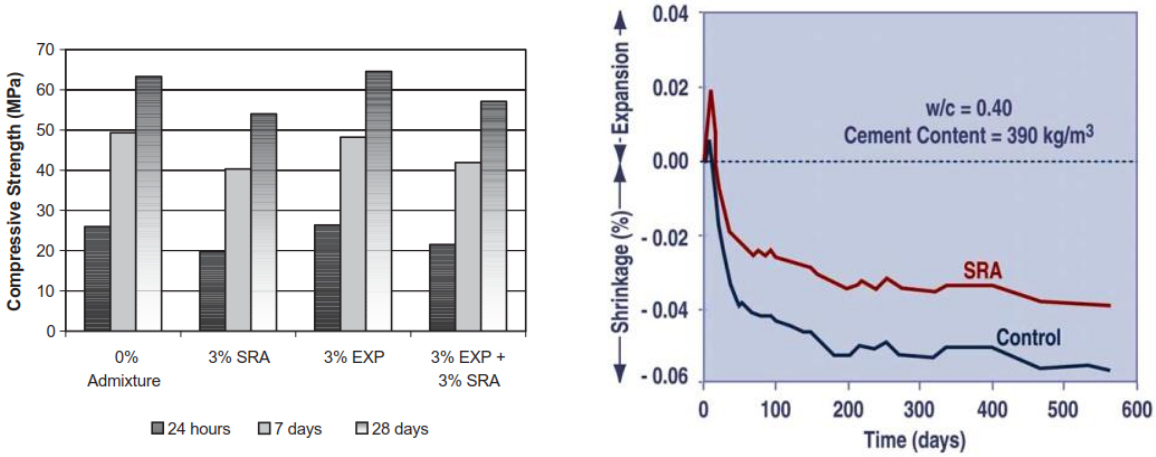

Figure 2.12 Shrinkage reductions with SRA similar to Sika Control 40. 390 kg/m^3 cement, 0.4 w/c and one week wet curing at 25 degrees Celsius. (Collepardi et al., 2005)

2.2.4.4 Downsides of applying SRA

As discussed above the application of SRAs can reduce drying shrinkage of concrete. However, the effects of applying SRAs are not limited to reducing shrinkage. Reported side effects of SRAs range from delayed hydration to strength reduction. Cerulli et al. (2001) used an isothermal heat flow calorimeter to observe the delay of the acceleration period and a delay time of maximum heat release when SRA was applied. Also, the heat of fusion increased with increasing amount of SRA. Both initial setting time and final setting time increased. Cerulli et al. (2001) and Maltese et al. (2005) both observed lower amounts of portlandite after 1 day of hydration. This is related to the lower rate of hydration observed with the isothermal heat flow calorimeter. A lower rate of hydration results in slower strength development compared to concrete without SRAs.

Shah et al. (1992) observed a decrease in the pore volume in the range of 50 nanometres to 10 micrometres. This was observed with the use of mercury intrusion porosimetry measurements. Due to an increase in low density CSH formation in the presence of SRA there was an increase in specific surface area and overall porosity. The downside is, that concrete with higher porosity is less durable and has lower strength than concrete with lower porosity.

The compressive strength in presence of SRA was investigated. An average decrease of compressive strength of 5-10% was observed with extremes up to 20% (Eberhardt, 2010). The flexural strength decreased by 10-15% with extremes up to 28% (Eberhardt, 2010). Splitting tensile strength was not affected. The tensile strength decreases in the range of 8-34% when SRA is applied. Creep resistance increased a lot. Drying creep reduction of up to 60% in compression and 39% in tension have been observed. The normal creep did not change. Due to less, smaller or no cracks at all the durability of the concrete improves (Eberhardt, 2010). Thus, applying SRA positively reduces drying shrinkage and crack formation but results in strength reduction.

Multiple authors report observed downsides for applying SRAs as stated above. Their focus, however, is relatively specific. Cerulli et al. (2001) and Maltese et al. (2005) focussed on the hydration process, Shah et al. (1992) observed changes in porosity and Eberhardt (2010) reported strength reduction of concrete. Further information about the mechanism of shrinkage reduction of SRAs, and information about influences of SRAs on hydration and mechanical properties divided per property is limited. Influences on the hydration process will affect the microstructure and subsequently the mechanical properties (Neville, 1995). But an overview about these relations with the mechanism of applying SRA as a basis is unavailable. Therefore, the focus of this research is to create an overview that describes, the mechanism of shrinkage reduction and the investigation of the SRA influences on the hydration process and mechanical properties.

2.3) Objectives

Shrinkage reducing agents can reduce drying shrinkage by lowering the surface tension of water. Reducing the surface tension results in lower capillary tension according to the Kelvin equation. Scientific information about the mechanism of shrinkage reduction is limited. Furthermore, a complete overview describing the side effects of applying SRAs on both the hydration process and mechanical properties is unavailable. Therefore, the objectives of this research are:

- Describe the mechanism of shrinkage reduction of Sika Control 40.
- Investigate the degree of shrinkage reduction.
- Investigate the influences on the hydration process and mechanical properties when applying Sika Control 40.

3) Methodology

To gain more insight into the influence of applying Sika Control 40 on the hydration process and on the mechanical properties of concrete, a series of experiments was performed. The performed experiments can be divided into two parts. Part 1 contains the experiments on cement paste samples and part 2 consists of the experiments on concrete samples. This division between experiments on cement paste and concrete was made because the tests on cement paste give insight into the hydration process and the tests on concrete give insight into the mechanical properties of concrete.

Table 3.1 gives an overview of the experiments performed. These specific experiments were chosen, because the combined results of calorimetry, porosimetry, surface tension, cement paste shrinkage and strength development give solid information on the hydration process of cement. Concrete compressive strength, concrete shrinkage and elastic modulus are important mechanical properties when constructing monolithic floors without dilation joints. With the combined results of these tests a well-rounded-recommendation and conclusion can be formed.

Table 3.1 Overview of performed experiments

Part I Cement paste	
	Surface tension of water
	Rate of hydration (calorimetry)
	Mercury intrusion porosimetry
	Autogenous and drying shrinkage
	Compressive strength
	Flexural strength
Part II Concrete	
	Compressive strength
	Autogenous and drying shrinkage
	Young's modulus

In this chapter each test setup of the experiments is described, and the related test method explained.

3.1) Test methods Part I: Cement paste

Five experiments were performed on cement paste. For these experiments four different mixtures were used with different amounts of SRA and one reference mixtures. In Table 3.2 the details of the mixtures are shown.

Table 3.2 Cement paste shrinkage mixtures (w/c=0,48)

Mixture	w% of cement SRA	Cement [g]	SRA [ml]	Deionized water [ml]	Total Fluid [ml]
ref	0	1000	0	480	480
052	0,52	1000	5,2	474,8	480
156	1,56	1000	15,6	464,4	480
261	2,61	1000	26,1	453,9	480

For these mixtures it is decided to use respectively 0.52 w%, 1.56 w% and 2.61 w% of cement SRA, based on the recommended applied concentrations specified by Sika BV. The minimum recommended concentration is 0.52 w% of cement, the maximum 2.61 w% of cement. 1.56 w% of cement is in the middle of these values. With these values, the influences of SRA concentrations can be investigated.

The name of the sample refers to the amount of shrinkage reducing agent applied in the mixture. 052 means that 0.52 of weight percentage of the cement is used in the mixture. This is similar for 156 and 261, here 1.56 and 2.61 weight percentage of cement respectively is applied. The ref mixture is the reference mixture without any SRA.

3.1.1 Surface tension

The first experiment on cement paste was performed to research the effect of different concentrations of Sika Control 40 on surface tension of water. The reason is that Sika Control 40 as an SRA actively lowers the surface tension of the mixing water of the mixture. Therefore, it is interesting to know to what extent the different concentrations reduce the surface tension. To determine this, four different mixtures were prepared and tested (see Table 3.3).

Table 3.3 Surface tension mixtures with w/c=0,48.

Mixture	SRA [ml]	Deionized water [ml]	Total [ml]
ref	0	100	100
052	1,08	98,92	100
156	3,24	96,76	100
261	5,43	94,57	100

The decision was made to use mixtures of deionized water with Sika Control 40 instead of pore solution with Sika Control 40. Pore solution is water from the pores of hardened cement. It contains a multitude of ions, for example OH^{---}, Cl^{-}, Na^{+} and K^{+} (Anstice et al., 2004). The decision to use deionized water was made because no interaction between the pore solution and Sika Control 40 was expected (Rajabipour, 2008).

Subsequently, the surface tension of the four mixtures was determined by using the Krüss Processor Tensiometer K100 (see Figure 3.1). For this a Krüss Standard Plate (width 19.9 mm / depth 0.2 mm / height 10 mm) was used for the measurements and the mixtures were placed in a glass vessel with a volume of 121.5 ml (see Figure 3.2).

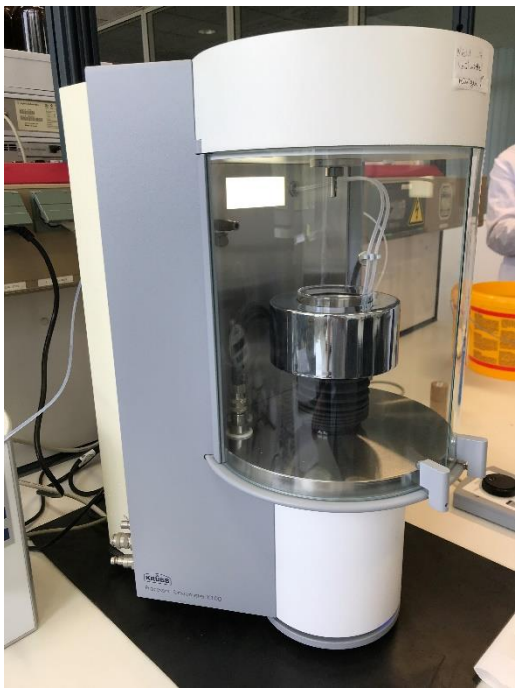

Figure 3.1 Krüss Processor Tensiometer K100

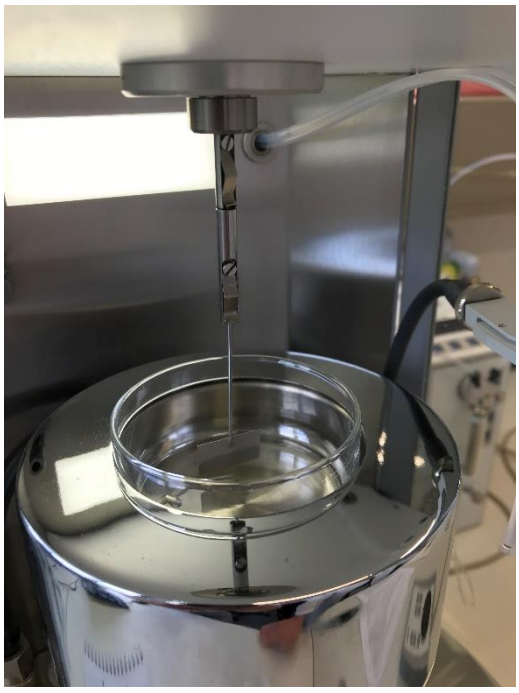

Figure 3.2 Glass vessel with Krüss Standard Plate

Before the test, the glass vessel was cleaned with isopropanol and double distilled water. The vessel was then pre rinsed with the mixture. A minimum of 35 ml of the mixture was then placed inside the vessel and the vessel was placed inside the tensiometer.

In addition, the Krüss Standard Plate was cleaned with isopropanol and double distilled water. Then, while rotating, the plate was dried above a Bunsen burner. After the plate glowed for a split second, it was placed in the mount of the weighing system of the tensiometer.

The last step, before performing the test, was to lift up the vessel to the point that the liquid surface was right below the Standard Krüss Plate. The Krüss standard plate was then lowered into the water and pulled back up. Due to the surface tension of the water the plate is pulled down. The Krüss Processor Tensiometer K100 measures this force of the water pulling on the plate. The accuracy of the K100 Tensiometer is 0.001 µN. As the size of the Krüss standard plate is known (width 19.9 mm / depth 0.2 mm / height 10 mm), the surface tension can be obtained. During 60 seconds the tensiometer performed ten individual measurements, resulting in an average surface tension value in mN/m. All above steps were repeated for the other mixtures.

3.1.2 Calorimetry measurements

The second experiment on cement paste involved calorimetry measurements to observe the rate of hydration and the heat of the hydration. For this experiment the four mixtures as described before were used.

Figure 3.3 Calorimeter setup

As the specific heat capacity depends on the weight of the cement paste, the sample weight was kept constant for each mixture. Approximately 5 grams of cement paste was advised per ampoule. A mass of 5.14 grams of cement paste was chosen to be placed in the glass ampoules. The water to cement ratio was 0.48 so this resulted in 1.67 grams of water and 3.47 grams of CEM III/B. Since the heat capacity must be matched with the reference ampoule containing quartz, the weight of the quartz was also calculated. The amount of quartz that is needed is calculated by using the C_p values of each material: $C_{p\ water}$=4.18 J/gK, $C_{p\ cement}$= 0.8 J/gK and $C_{p\ quartz}$=0.75 J/gK[1]. As a result, 12.99 grams of quartz were used in the reference ampoule.

After the preparation of the ampoules with either cement paste or quartz, the ampoules were placed in the calorimeter. During seven days the heat exchange of the ampoules with the environment was closely measured by the calorimeter. In this way the heat of hydration over time was observed, which is a measure for the rate of hydration. In addition, the total cumulative heat can be related to the degree of hydration over the first seven days. One measurement per sample was performed. Due to the good reproducibility of the calorimetry experiment one measurement per sample was sufficient.

[1] According to the data sheet the C_p of Sika Control 40 was similar to that of water (Sika Group, 2014). Because it replaces a part of the mixing water but does not change the total amount of water it is not noted separately.

3.1.3 Mercury intrusion porosimetry

The third experiment was the porosity test. For this test cement paste samples were prepared for the four mixtures. For each mixture three samples were prepared for testing after 1, 7 and 28 days of hydration. One measurement per sample was performed, due to the good reproducibility of the test method one measurement was sufficient.

Preparation of samples

At first, the samples were mixed and cast into small plastic cups and covered with watertight foil before the lid was screwed back on. In this way no water could escape the bottle. After one day of hydration the first batch of samples (one sample of each mixture) was opened and broken with a hammer to obtain small fragments of a few millimetres in size. Fragments that were in contact with the side of the plastic bottle were discarded because this might have affected the porosity. The suitable fragments were then submerged in liquid nitrogen to freeze them thereby stopping the possibility of further hydration.

Figure 3.4 Sample bottles sealed with watertight foil

Subsequently, the frozen fragments were placed in a sample bag with small holes and then placed in the vacuum dryer. The vacuum dryer ensured that the ice immediately evaporated instead of melting first. In this way no further hydration occurred.

Lastly, the samples were weighed regularly over weeks to months to follow the weight loss. When the weight loss was less than 0.05 grams per day the samples were considered dry and the pores empty. After this, the samples were ready to be analysed in the mercury intrusion porosimeter.

The above explained process was repeated after 7 days of hydration and after 28 days of hydration.

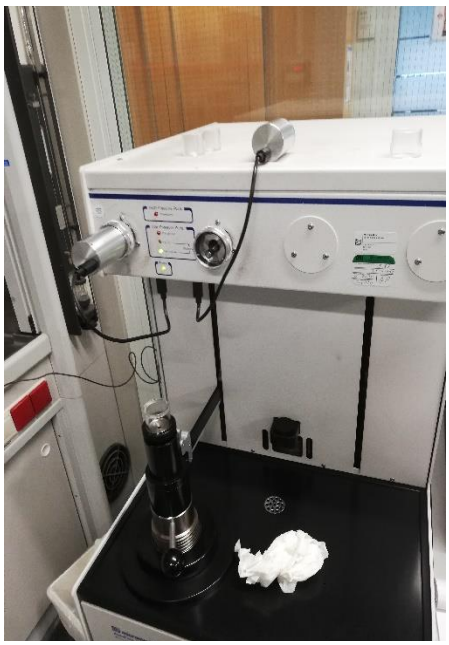

Figure 3.5 Mercury intrusion porosimeter

Preparation for the mercury intrusion porosimeter

To prepare the dried samples for testing with the mercury intrusion porosimeter, approximately 3 grams of fragments were obtained. This amount was then placed in the glass container part of the penetro. The penetro is a metal straw with a glass sample container attached on one side. Following, an airtight seal was applied on the top edge of the glass penetro before placing the lid and fastener. Also, vaseline was applied to the bottom 4 cm of metal of the penetro to ensure a good seal with the rubbers inside the machine. The metal part of the penetro was inserted into the porosimeter and the penetro was tightened before the test could start.

The mercury intrusion porosimetry test

First a vacuum was created by the porosimeter to ensure that no air remained in the sample and sample container. When the threshold of 60 µmHg was reached and maintained for 10 minutes, the mercury was inserted via the metal part of the

penetro into the sample container to make contact with the sample.

Subsequently, the penetro with the sample and inserted mercury was extracted and weighed and then placed in the high-pressure chamber. Then the pressure was increased periodically and during this the volume of the inserted mercury was measured. When the maximum applied pressure of 210 MPa was reached, the pressure was reduced again to extract the mercury with suction. After the mercury was extracted the penetro with the sample was removed from the porosimeter and the test was complete. After the penetro was rinsed and cleaned the next sample could be tested.

3.1.4 Autogenous and drying shrinkage of cement paste

The fourth experiment was to investigate the shrinkage of the cement paste. It was decided to test the autogenous shrinkage over the first seven days after casting and to test the drying shrinkage from seven days onwards. To achieve this the samples were wrapped in watertight foil for seven days to prevent water loss. After those seven days the samples were unwrapped and thus exposed to air to dry, which started the drying shrinkage measurement.

Preparation of samples

For testing the shrinkage for each of the four mixtures three prisms (rectangular bars) of 4x4x16 cm were cast in foam moulds. Immediately after casting the prisms were covered with plastic to prevent evaporation of water and to minimize plastic shrinkage. After one day of hydration the prisms were demoulded and wrapped in watertight duct tape and the casting side was marked for reference. When the prism was wrapped, two points on the left and right side of the prisms with respect to the casting side were marked. These points were 3 cm from top and bottom and 2 cm from the front- and rear sides. This resulted in two points on each side, that were located 10 cm from each other.

Figure 3.6 Cement paste autogenous shrinkage setup. Sample is wrapped in watertight tape and measuring clocks are attached.

Next, the duct tape on these positions was cut away to expose the hardened paste. Mounts were then glued directly on the bare paste, which supported the clocks for measuring the shrinkage. Once the mounts were glued the clocks were attached in such a way that the clock was fixed in the top mount and the metal rod in the bottom mount. This had as a result that when the prism changed length the metal rod was able to move in or out of the clock to show shrinkage or expansion on the clock.

In Figure 3.6 the complete setup of one prism can be observed. The picture shows the wrapped version of the prism, the setup for testing the autogenous shrinkage. After the first seven days, the tape was removed while maintaining the mounts in place.

Measurements of autogenous and drying shrinkage

After the clocks were attached to the prisms, the clocks were adjusted to a reading of 5.00, which is in the middle of its range to allow both shrinkage and expansion. One full rotation on the clock meant one centimetre length change. With each rotation divided into 100 parts (meaning an accuracy of 0.1mm) a good estimation could also be made for the value between two parts, so results were noted with 0.01 mm accuracy. In the first couple of days measurements were performed twice a day. In the weeks after, this was reduced to daily measurements to be able to precisely follow the shrinkage.

As two clocks were used per prism to counter possible curving of the prism, the average was taken of both clocks to obtain the shrinkage value of one prism. Thereby, every time the shrinkage values were

noted, each prism[2] was weighed to follow the loss of water in the prisms; For this, a scale with an accuracy of 0.1 gram was used.

3.1.5 Flexural strength

The fifth experiment with cement paste was the flexural strength measurement. This was done with similar prisms as for the shrinkage measurements. These prisms were also cast in the foam moulds and covered immediately after casting to prevent evaporation of water and minimize plastic shrinkage. Each of the four mixtures were tested on three prisms at each test moment, which took place after 1, 3, 7, 14 and 28 days of hydration. One day after casting all prisms were demoulded. The prisms needed for the one-day test were directly tested. The other prisms were placed in the curing room at 20 ^{o}C and 95% relative humidity for later testing.

Figure 3.7 Left: broken flexural strength prisms; Right: Prisms ready for testing

The flexural strength was tested with a three-point bending setup. The setup had a span of 10 cm and a force on the prism was applied in the middle of these supports with a hydraulic press. The prisms were placed with the casting side positioned sideways. Subsequently, a loading speed of 0.05 kN/s was applied to the prism. The load was increased until the prisms broke. The flexural strength was then calculated from Equation 4:

$$\sigma_f = \frac{3FL}{2bd^2}, \qquad \text{Equation: 4}$$

where σ_f is the flexural strength of the prism, F is the applied force at failure, L is the span between the supports, b is the width of the prism and d is the depth of the prism.

[2] Including the clocks.

3.1.6 Compressive strength

The last experiment on the cement paste was performed to measure the compressive strength. For this test the same prisms were used as for the flexural strength test. The prisms were broken into two parts during the execution of the flexural strength tests. Due to the three-point bending setup that was used, all prisms were approximately broken in half. These two parts were then used for the compressive strength test.

Figure 3.8 Paste compressive strength samples

Figure 3.9 Compressive strength sample after failure

The compressive strength test was performed with the same hydraulic press as the flexural strength test only a different mount was used. The halved prisms were positioned with the casting side pointed sideways. Then, the 4x4 cm area was compressed. This area was located 5mm from the unbroken side of the prism to ensure that the compression zone had not been loaded before. A loading rate of 2.4 kN/s was used, and measurements started at 2 kN. The prisms were compressed to failure to obtain the maximum load. This translated to the maximum compressive strength in MPa by:

$$\sigma = \frac{F}{A}, \qquad \text{Equation: 5}$$

where σ is the compressive strength in Pa, F is the maximum load at failure in N and A is the compressed area in mm^2 (here $1600mm^2$).

3.2) Test methods Part II: Concrete

Now that the cement paste experiments were completed and analysed, it was time to scale up to concrete specimens. It was chosen to test the compressive strength, shrinkage, and the Young's modulus of concrete. For each experiment, the same mixture has been used. Similar to the cement paste experiments four different mixtures were created with the SRA concentration as the only difference. In Table 3.4 the mixture designation can be found. Per mixture, 36 cubes of dimension 15x15x15 cm and 24 rectangular prisms of dimensions 10x10x40 cm were cast. The 36 cubes were used for the compressive strength tests, 12 of the prisms were for the shrinkage experiments and the other 12 prisms were used for the Young's modulus experiments.

Table 3.4 Concrete mixtures (w/c=0.48)

Mixture	CEM III/B [kg/m^3]	Sand 0-4mm [kg/m^3]	Gravel 4-16mm [kg/m^3]	Gravel 4-32 mm [kg/m^3]	SRA [kg/m^3]	Water [kg/m^3]
ref	350	735	367,5	735	0	168
52	350	735	367,5	735	1,82	166,18
156	350	735	367,5	735	5,46	162,54
261	350	735	367,5	735	9,14	158,87

Preparation of cubes and prisms

On the day of casting the moulds were cleaned and oiled to ensure that the samples came out complete and clean. All the cubes and prisms for one mixture were cast at once. Thereafter, the concrete samples were covered with plastic foil to reduce evaporation and thereby minimizing the plastic shrinkage. The same procedure was repeated for the other mixtures.

The covered samples were then stored for one day in the casting room. After one day of hardening, the samples were demoulded. A number of the samples was used for the first experiments, the other samples was placed in the curing room. The curing room was climate controlled to be 20 degrees Celsius and 95% relative humidity.

Figure 3.8 Cast concrete prisms. Prisms are labelled and sealed with plastic foil until demoulding.

3.2.1 Compressive strength

The first concrete experiments were performed to test the compressive strength. For each mixture this was done after 1, 7 and 28 days of hydration. At each test moment, three cubes per mixture were tested. As done with the cement paste sample, the concrete cubes were compressed using a hydraulic press. The casting side was again orientated sideways to ensure that the pressed sides are smooth, and the forces were exerted homogeneously. A loading rate of 13.5 kN/s was used, and the cubes were compressed until failure, to obtain the maximum compressive strength.

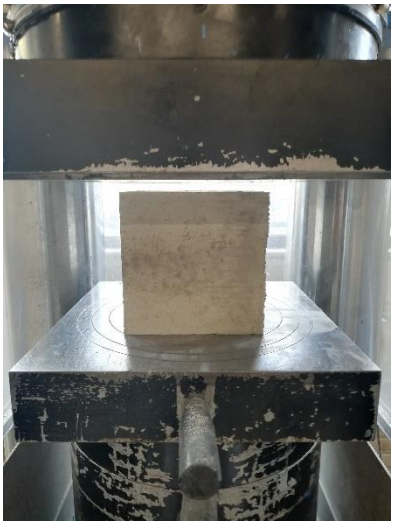

Figure 3.9 Concrete cube before compression test. Cube is faced sideways and positioned in the center of the press.

Figure 3.10 Concrete cube after compression test.

3.2.2 Free shrinkage of concrete prisms

The second experiment performed on the concrete samples was to test the free shrinkage of the concrete prisms. A similar approach was used for testing on the concrete prisms as was used for testing on the cement paste prisms. Again, three prisms were cast per mixture. In addition, it was again decided to start by measuring the autogenous shrinkage during the first 7 days of hydration and the drying shrinkage after the first 7 days.

Therefore, the prisms were demoulded after one day of hydration and after marking the casting side, the prisms were wrapped in watertight bitumen tape. The seams between the bitumen tape were sealed with duct tape. Subsequently, the location for the mounts were marked on the left and right side of the prism. The mounts were located 10 cm from top and bottom and 5 cm from front- and rear sides. This way the mounts were located 20 cm from each other. On these locations the tape was cut away and the metal mounts were glued onto the bare concrete. Once the glue hardened the clocks were attached and adjusted to a reading of 5.00, which is halfway its range. Like the cement paste samples, two dial clocks were used on opposite faces to account for possible curving of the prism. The average of both dial clocks was the value used for the shrinkage measurement. The same clocks were used as in the cement paste shrinkage experiment resulting in similar accuracy of 0.01 mm.

After 7 days the bitumen tape was removed from the prisms, exposing them to the air and starting the drying shrinkage. The bitumen tape was precisely cut away around the mounts to make sure the clocks did not break off, so the measurements would continue. The bitumen tape was difficult to remove and left a brownish colour on the surface of the prism. Although not visually pleasing it did not harm the prisms.

To check the loss of water the prisms were weighed every time the shrinkage values were noted. A scale with an accuracy of 0.1 g was used. During the first 3 days, two measurements were performed, after that measurements were performed daily in the first couple of weeks.

Figure 3.13 Concrete autogenous shrinkage setup. Prism is sealed with bitumen foil and duct tape. Two measuring clocks are attached on opposite sides per prism.

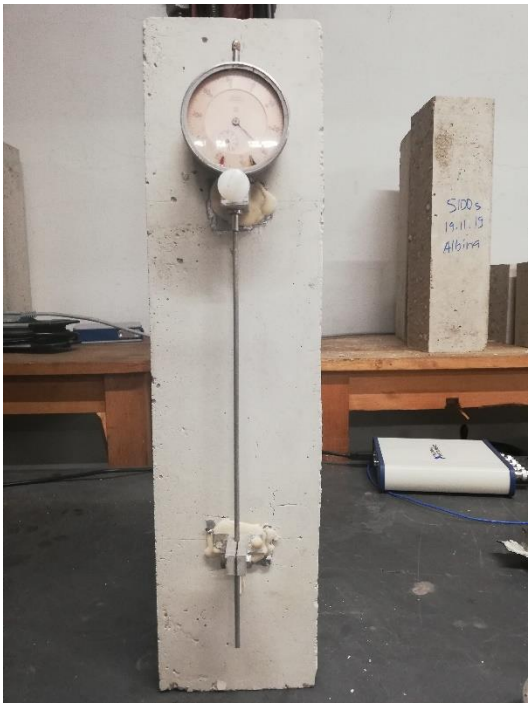

Figure 3.14 Concrete drying shrinkage setup. Prism is exposed to the air after removal of bitumen foil.

3.2.3 Elastic modulus

The final experiment performed on concrete samples was the elastic modulus test. For this test also 12 prisms were used. Again, three prisms of each mixture were tested. As testing elastic modulus is time-consuming, it was decided that the test would be performed only after 28 days of hydration.

The elastic modulus was obtained by measuring the change in length of the prism while being compressed. The length change was measured by LVDTs. For using these LVDTs they need to be placed in mounts that are glued to the concrete prism. In Figure 3.16 the glued mounts can be observed. The mounts facilitated the placement of one vertical and one horizontal LVDT on each side of the prism. The vertical LVDTs measure the length change, which was used to calculate the elastic modulus of the concrete. The horizontal LVDT measures the change in width of the prism to calculate the Poison's ratio of the concrete.

After attaching the mounts, the prism was placed in the compression machine and the LVDTs were placed and fastened in the mounts. The hydraulic press then started to compress the prism in a strain-controlled mode with a speed of 0.0010 kN/s. With the force of the press and the length change of the LVDTs the elastic modulus and the poisons ratio were calculated using the average of the 4 respective LVDT's.

Figure 3.11 Elastic modulus test with attached LVDT's

Figure 3.16 Prism with glued mounts for LVDT's

4) Test results and discussion

In this chapter an overview of the test results will be given. Results of each experiments will be discussed separately.

4.1) Test results Part I: Cement paste

First the test results on the cement paste samples will be given, starting with the surface tension experiments.

4.1.1 Surface tension measurements

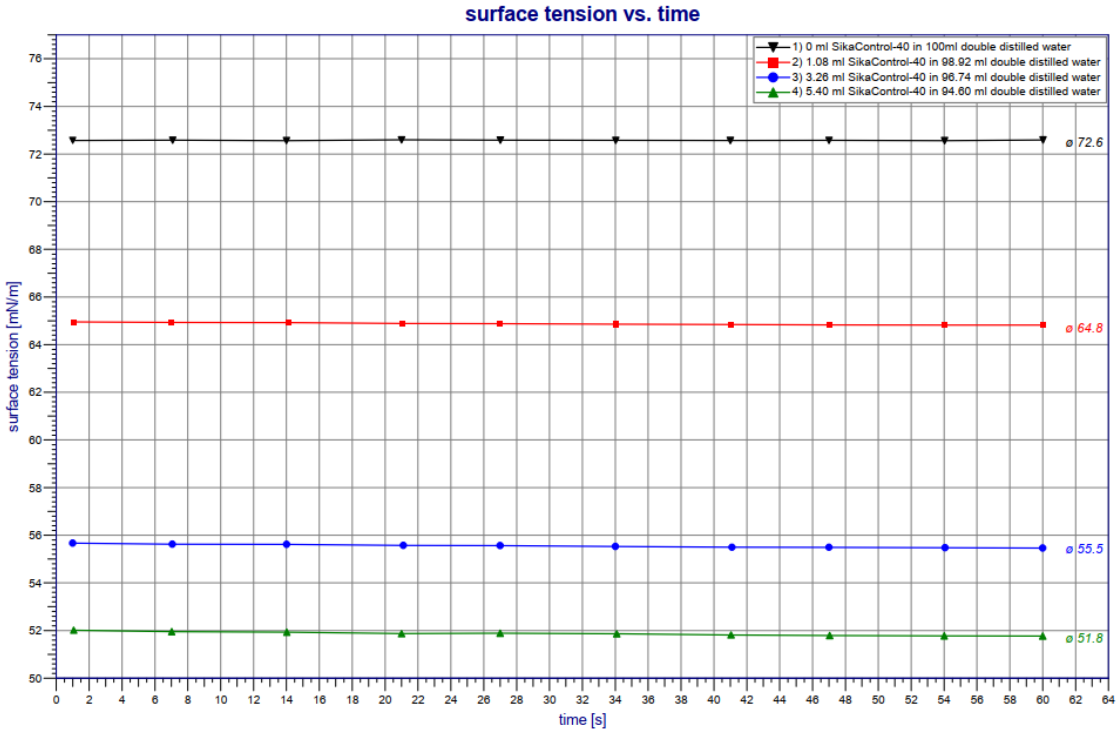

Figure 4.1 Surface tension results. Reference (Black, 0 w% SRA) averages at 72.6 mN/m, 052 (Red, 0.52 w% SRA) averages at 64.8 mN/m, 156 (Blue, 1.56 w% SRA) averages at 55.5 mN/m, 261 (Green, 2.61 w% SRA) averages at 51.8 mN/m.

Four mixtures were analysed with a Krüss Processor Tensiometer K100. Over the duration of one minute ten measurements were performed. The results can be observed in Figure 4.1. The reference sample (black) had an average surface tension of 72.6 mN/m. The 052 (red), 156 (blue), 261 (green) samples had averages of 64.8 mN/m, 55.5 mN/m, and 51.8 mN/m, respectively. When the decrease in surface tension is compared to the amount of SRA that was applied, no linear relation was found. 0.52 w% SRA lowered the surface tension by 10.7% with respect to the reference sample. For concentrations of 1.56 w% and 2.61 w% the surface tension decreased by 23.6% and 28.7% with respect to the reference sample. Increasing the SRA concentration had diminishing returns on the surface tension reduction. This is caused by the nature of surfactants. Due to the hydrophilic and hydrophobic chain, surfactants will position themselves on the interface of the water with another liquid, solid or gas. The hydrophilic part points towards the water by forming hydrogen bonds and the hydrophobic part points itself towards the other medium (Rosen, 2004). However, a certain threshold exists for the concentration of surfactant in the solution. When this threshold is reached the surfactant

will start to form micelles in the solution. This is called the critical micelle concentration (CMC). When the CMC is exceeded more SRA could still be added but the effectivity of the extra surfactant drastically decreases. This behavior was observed in the results. 0.52% SRA reduced the surface tension by 10.7%. When 1.56 w% was added, which was three times the amount, the surface tension did not decrease by 10.7*3=32.1% but only by 23.6% which is 2.21 times as much. The effect was even more pronounced for the 2.61 w% SRA. With respect to 0.52 w% almost five times more SRA is applied but it only reduced the surface tension by a factor of 2.68.

Table 4.1 Surface tension results and their decrease with respect to the reference sample.

	w% of cement SRA	Surface tension [mN/m]	Decrease [%]
ref	0	72,6	-
052	0,52	64,8	10,7
156	1,56	55,5	23,6
261	2,61	51,8	28,7

4.1.2 Isothermal calorimetry (hydration rate)

The typical rate of hydration graph for cement can be divided into five parts. Stage 1 is the initial dissolution part. From the moment the water is added to the unhydrated cement, cement starts to dissolve. A large decrease in heat flow can be observed. Stage 2 is the induction phase this is a period of slow reaction. Followed by a large acceleration in heat flow in stage 3 which relates to the fast formation of hydration products. Stage 4 is the deceleration stage. A lot of the cement particles have reacted with the water. This forms a layer of hydration products on the surface of the cement particles. This forms a sort of barrier along the cement particle making it harder for water to reach the unhydrated cement. This results in slower hydration and a decrease in heat flow, this can be observed in the graph as the deceleration in stage 4. In stage 5 slow continued hydration will continue.

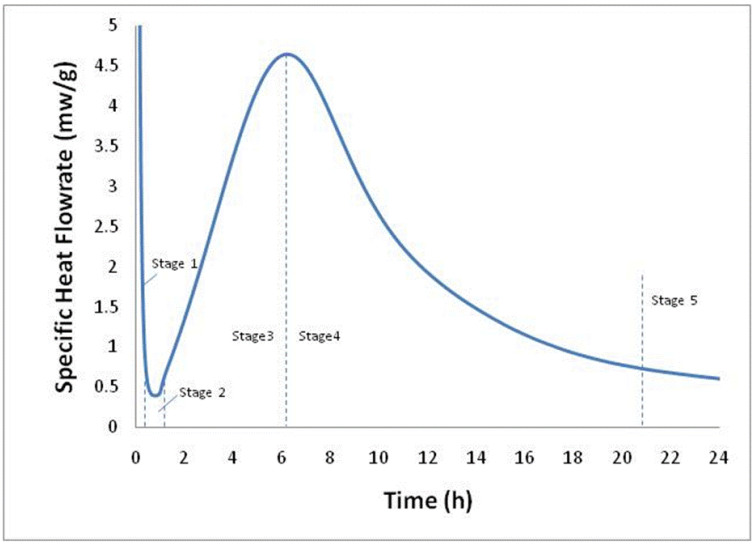

Figure 4.2 Specific Heat Flowrate during cement hydration process (Wadso, n.d.)

The amount of specific heat that is emitted is a measure for the degree of hydration. This can be expressed in the cumulative heat. A characteristic cumulative heat curve is shown below.

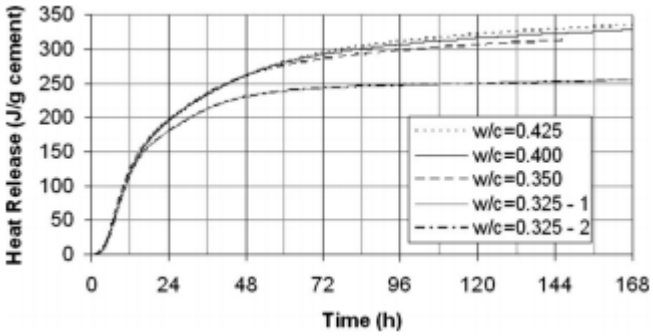

Figure 4.3 Cumulative heat curve of cement hydration for w/c ranging between 0.325-0.425 (Bentz, Peltz, & Winpigler, 2009)

For the calorimetry test cement specimens were made with different SRA concentrations (0, 0.52, 1.56, 2.61 w%) which were tested for 7 days. This way the hydration rate and degree of hydration was obtained for different SRA concentrations.

All four samples were prepared in quick succession and the calorimetry test was started immediately after the samples were cast. The test started at the same time for all mixtures. The heat flow curves of the four different mixtures are shown in Figure 4.4. The vertical axis shows the heat flow in watt and the horizontal axis shows the time in hours. The total time was 7 days. The shape of all the curves followed the expected path of a typical heat flow curve as described and shown in Figure 4.2. However, it was observed that there is a shift between the different curves. Especially when the two different peaks were compared. Not only the timing of the peaks was different but the height as well. When more SRA was applied in the mixture, the peaks of the heat flow curves were delayed, and peak heat flows were lower. This effect was more pronounced for the mixtures with 0.52 w% and 2.61 w% than for the 1.56 w%. It would be expected that the 1.56 curve was approximately in the middle between the 0.52 and 2.61 curves, but it was closer to the 0.52 curve. From these results it was concluded that the rate of hydration was lowered when SRA is applied.

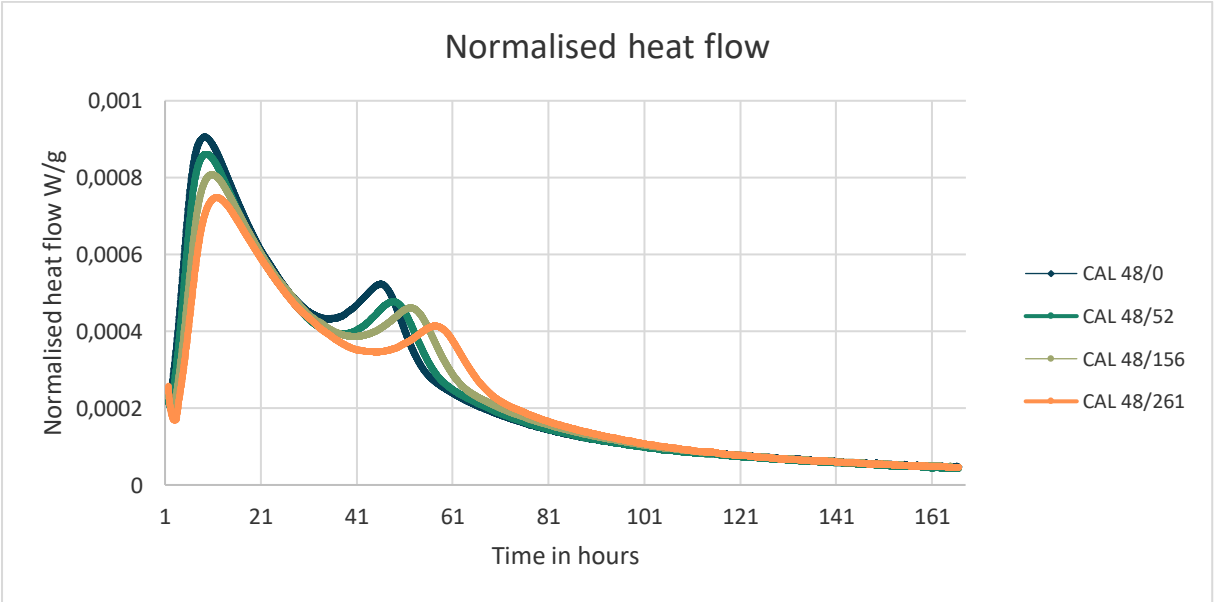

Figure 4.4 Heat flow curves of cement hydration of CEM III/B with w/c=0.48 during the first 7 days of hydration. CAL 48/0 (blue) is reference (0 w% SRA), CAL 48/52 (dark green) is mixture 052 (0.52 w% SRA), CAL 48/156 (light green) is mixture 156 (1.56 w% SRA), CAL 48/261 (orange) is mixture 261 (2.61 w% SRA).

The normalized cumulative heat of the four mixtures was compared as well. In the heat flow diagram, it was observed that the rate of hydration was affected by the SRA. The cumulative heat curve showed that the total heat of hydration was also lower for the mixtures with SRA when compared with the reference sample. The curves of the mixtures with SRA were similar but the heat of hydration was about 8 J/g less after 7 days of hydration. While the heat of hydration can be used as a measure for the degree of hydration, it was concluded that the SRA affected not only the rate of hydration but also the degree of hydration.

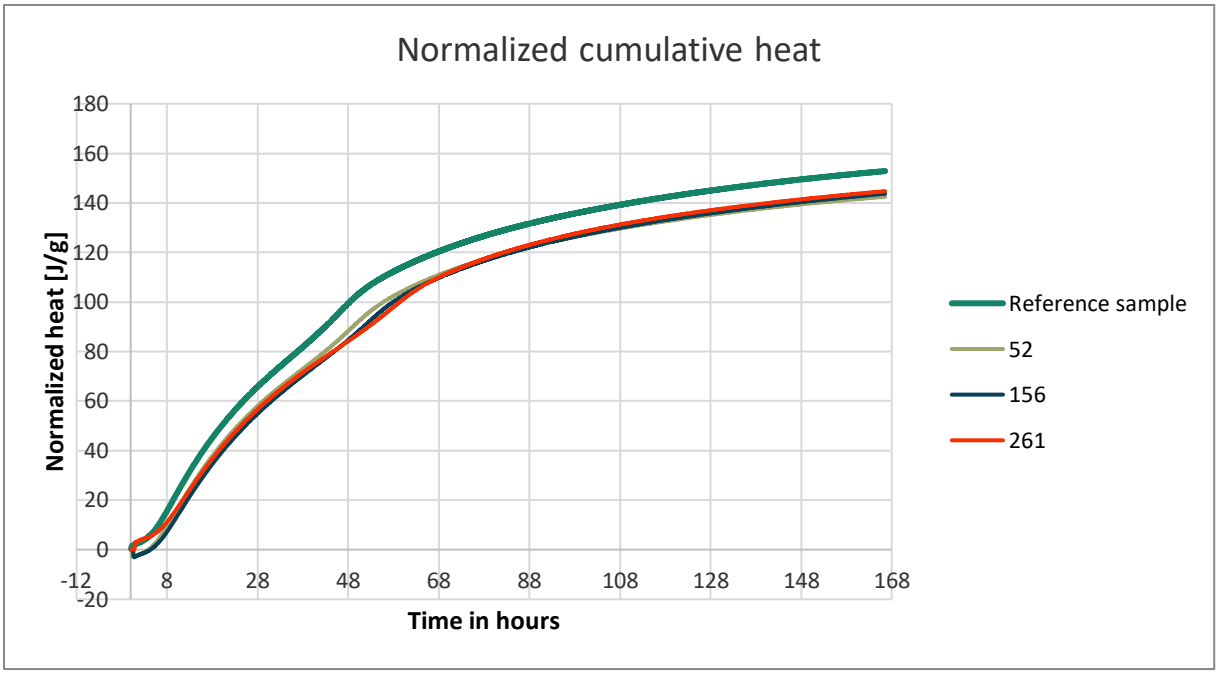

Figure 4.5 Normalized cumulative heat in [J/g] of cement hydration of CEM III/B with w/c=0.48 during the first 7 days of hydration. Reference: Red, 0 w% SRA, 052: Green, 0.52 w% SRA, 156: Blue, 1.56 w% SRA, 261: Orange, 2.61 w% SRA.

It was surprising that the SRA influenced the hydration rate in this matter.

Exploration of divergent results: Why the SRA affects the rate and degree of hydration is a very interesting question. The answer is not obvious and to determine why this phenomenon occurred the variables in the calorimetry test were examined. All the samples were prepared in a very close timespan. Their weight was normalized with the heat capacity of the quartz, so all samples are comparable with each other and results are normalized. The water to cement ratio was constant for all mixtures and the environmental conditions were constant as well, which rules out the influences of the environment and the mix design, except for the influence the SRA might have. As already mentioned in this thesis, the surfactant will position itself on the interface of the water and other liquids, solids, or gasses. This behaviour can be explained by their chemical configuration. The hydrophilic part forms hydrogen bonds with the water and hydrophobic chains can interact with the other media (Rosen, 2004). If we take a step back to the foundations of cement hydration then we can describe this as the dissolution of the cement particles in the added water and the formation of calcium silicate hydrates, calcium hydroxide and multiple other minerals. But for any of this to happen the cement should be able to dissolve in the water. When this does not happen then the cement hydration will also not occur. When we combine this fundamental process with the fact that surfactants position themselves on the interfaces of water with other liquids, solids or gasses because this is energetically most favourable, then it could possibly be explained why SRA reduces the rate of hydration and degree of hydration. If the SRA positions itself in between the water and the un-hydrated cement particles, then it forms a barrier in the hydration process. When concentrations of SRA are small then this effect

will be smaller than for larger concentration of SRA due to the simple fact that more SRA is able to form more of these interface barriers. This explains the lower rate of hydration because less cement can dissolve and hydrate than when there is no SRA. But it also explains the lower degree of hydration. As mentioned before the SRA is not expected to react with any of the materials in the mixtures. Therefore, the SRA will not decrease in amount due to dissolution and chemical reaction. Some SRA might be lost due to slight bleeding behaviour and evaporation, but this is minimal. Therefore, the SRA will remain in the hardened cement paste and concrete. It may also keep on shielding cement particles from contact with water. Especially when more and more water has reacted with the cement, less water remains for the SRA to position itself as energetically as possible. So, the same amount of SRA is on the interface of increasingly less water making it more difficult for the water to come in contact with the remaining un-hydrated cement. Resulting in a lower degree of hydration.

4.1.3 Cement paste shrinkage

In order to measure the shrinkage of the cement paste four different mixtures were prepared and cast into small prisms. Mix designs were like the mixtures that were used for the other cement paste experiments.

During the first 7 days of hardening the samples were wrapped and placed inside a climate chamber with a steady temperature of 20 degrees Celsius and a relative humidity of 50%. During these 7 days the autogenous shrinkage and the weight loss was measured daily. Because of the foil no water could evaporate the first 7 days therefore the occurring shrinkage was autogenous shrinkage. By measuring the weight of the samples, it was checked that no water evaporated. After 7 days the cement paste samples were unwrapped and exposed to drying to the air under similar environmental conditions. From this moment on water could evaporate and the drying shrinkage was measured as well as the weight loss of the samples.

By using this method, it was observed what the effect of different concentrations or SRA was on the autogenous shrinkage, drying shrinkage and on the weight loss of the samples. Figure 4.6-4.9 show the weight loss and the total shrinkage over time.

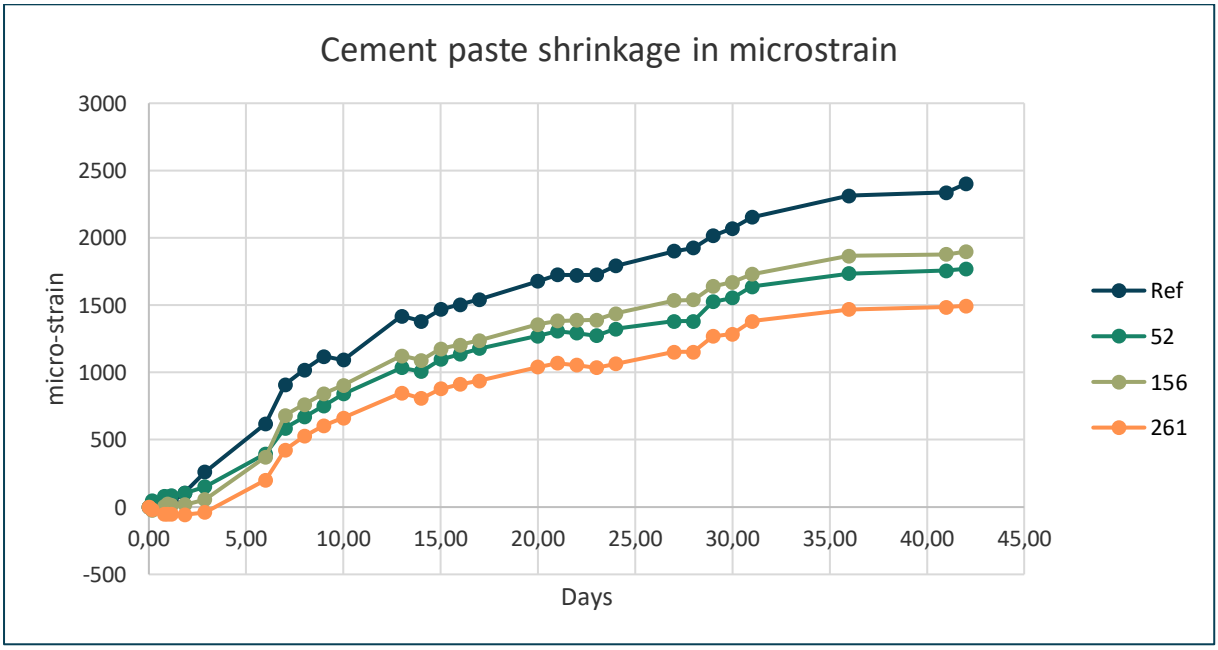

Figure 4.6 Cement paste CEM III/B and w/c=0.48 autogenous + drying shrinkage . First 7 days no loss of water, from day 7 onwards samples were exposed to drying. Ref=Blue, 0 w% SRA, 52=Dark green, 0.52 w% SRA, 156=Light green, 1.56 w% SRA, 261=Orange, 2.61 w% SRA.

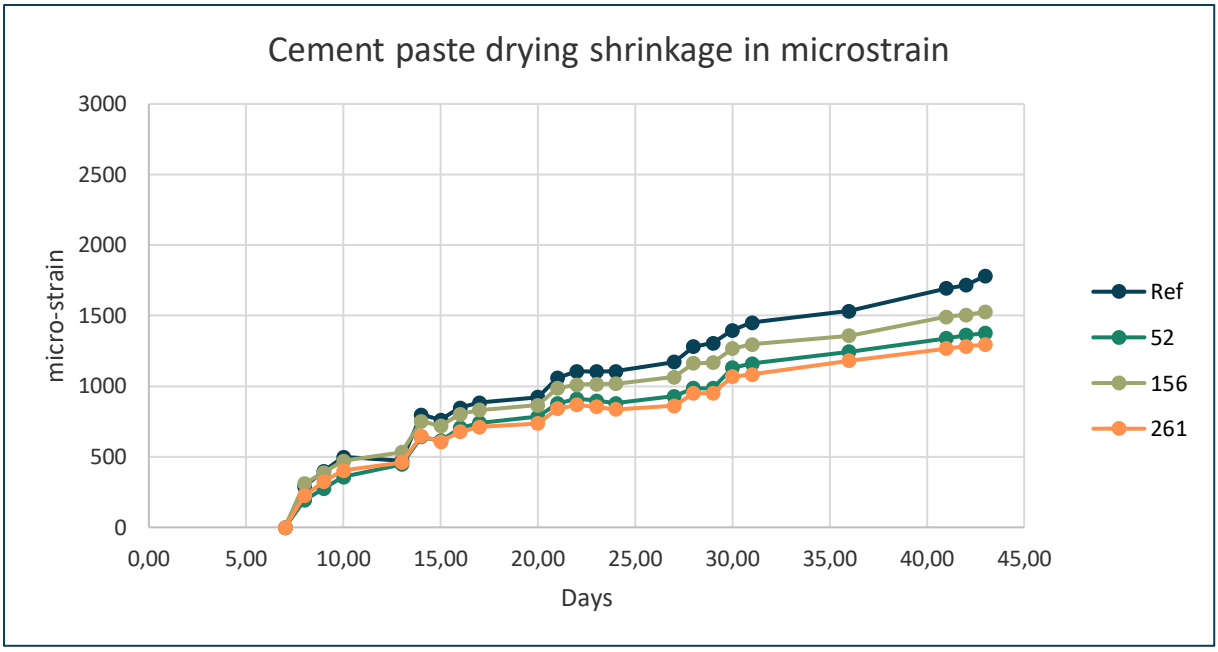

Figure 4.7 Cement paste CEM III/B and w/c=0.48 drying shrinkage in micro strain starting at moment of unwrapping. Ref=Blue, 0 w% SRA, 52=Dark green, 0.52 w% SRA, 156=Light green, 1.56 w% SRA, 261=Orange, 2.61 w% SRA.

In Figure 4.7 the drying shrinkage can be observed. Drying shrinkage is plotted from the moment of unwrapping therefore shrinkage starts at 7 days. The reference sample shrank most at every moment. It was as expected that a higher concentration of SRA would result in lower shrinkage. From the results it was observed that the sample with 2.61 w% SRA had the lowest shrinkage from day eight after unwrapping (day 16 after casting). During the first seven days after unwrapping sample 52 had the lowest drying shrinkage. During the first three days after casting sample 261 showed slight expansion. The samples with 0.52 w% and 1.56 w% SRA showed lower shrinkage than the reference sample and more shrinkage than the 261 sample as expected. These two samples were however swapped around with respect to the expected outcome. During the first 7 days the shrinkage pattern was completely as expected but after unwrapping the samples, the 156 sample overtook the 52 in shrinkage.

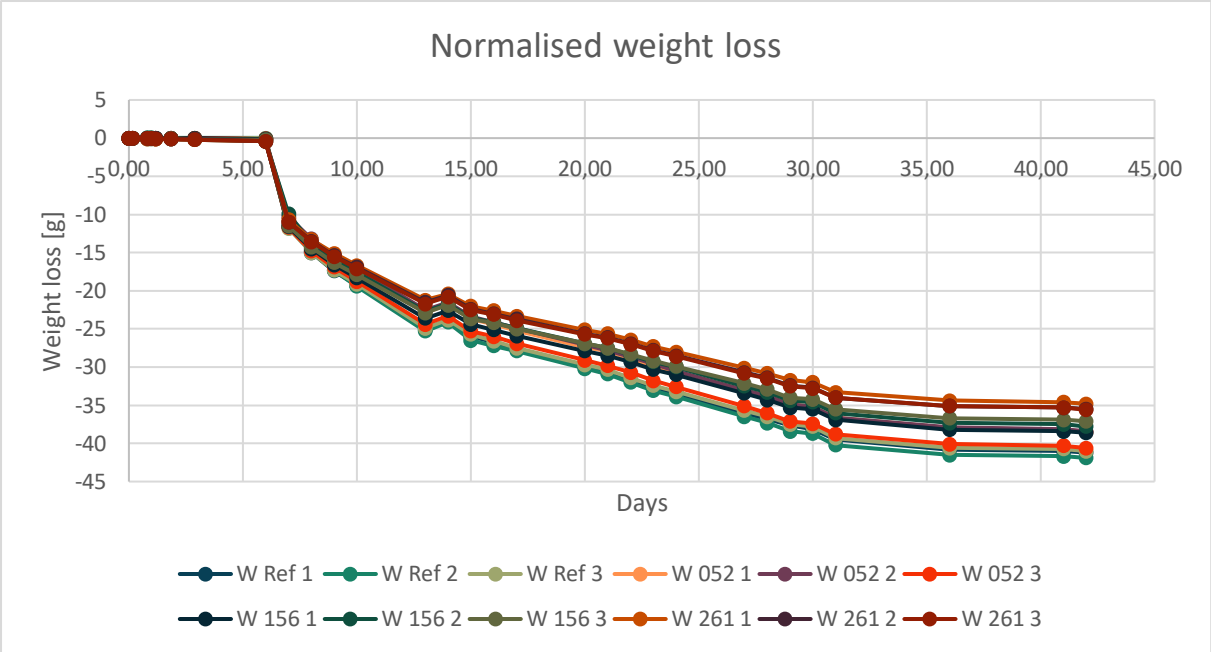

Figure 4.8 Normalised weight loss in gram per sample. Ref=0 w% SRA. 052=0.52 w% SRA, 156=1.56 w% SRA, 261=2.6 1w% SRA

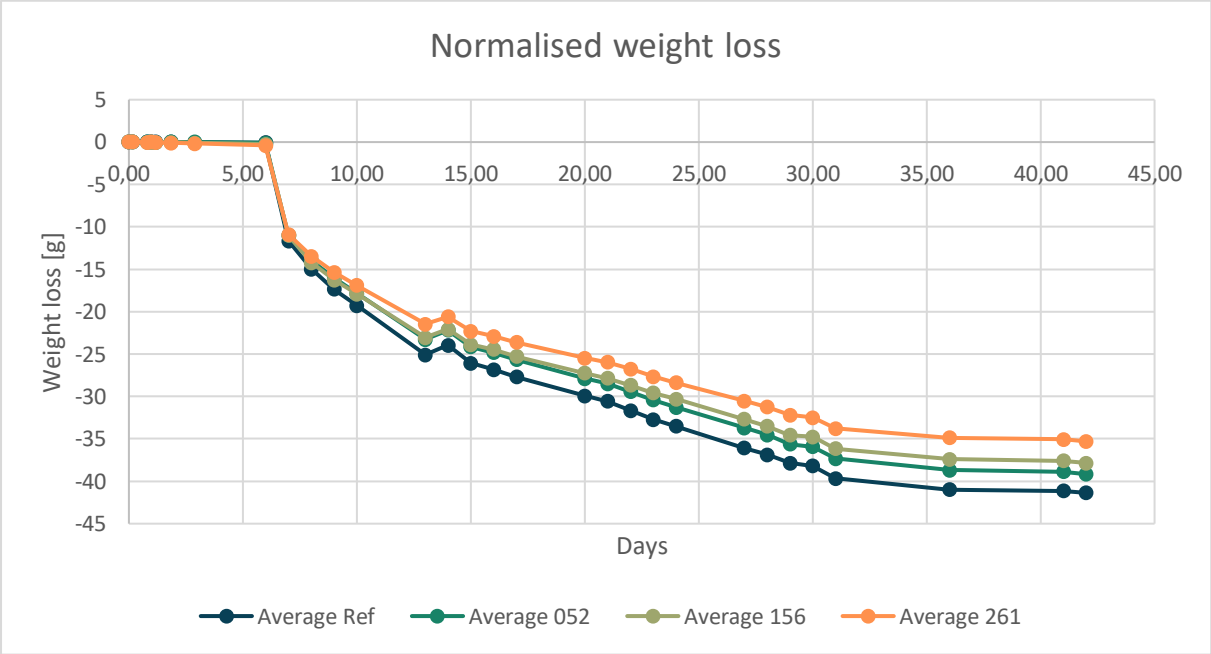

Figure 4.9 Average cement paste weight loss per mixture. Average Ref: Blue, 0 w% SRA; Average 052: Dark green; 0.52 w% SRA; Average 156: Light green, 1.56 w% SRA; Average 261: Orange, 2.61 w% SRA.

In Figure 4.8 and Figure 4.9 the weight loss of the samples is shown. During the first seven days, when the samples were wrapped, there was no weight loss in any of the samples. So, during the first seven days indeed autogenous shrinkage was measured. After unwrapping at 7 days all samples started to dry and became significantly lighter over time. The prisms without the clocks after demoulding weighed approximately 460 grams. The average weight loss per mixture was, 41.37 g; 39.17 g; 37.83 g and 35.3 g for Ref, 52, 156 and 261, respectively. This corresponds to a weight loss of the prisms of 7.5%-9% of its starting weight. The results showed that more SRA reduced the water evaporation. This could result in a lower drying shrinkage because the pores of the paste are less empty and, therefore,

the capillary tension is lower. Over time the cement paste increases in strength due to ongoing hydration. Due to strength increase, shrinkage will be lower, so even if the samples with more SRA may continue longer with evaporation of water, this will have a lower effect on the drying shrinkage. Combining the weight loss with the shrinkage graphs of 52 and 156 did not explain why 52 had less shrinkage then 156. Because the weight loss of mixture 052 was higher than 156 it would be expected that mixture 52 would shrink more than mixture 156.

An interesting point in the weight loss graph was at day 14. A sudden increase in weight was observed. And when the shrinkage graph was investigated closely a slight expansion was observed on day 14 for all the samples. This was curious but had a simple explanation. There was a slight malfunction in the climate control of the room and as a result of that the relative humidity increased suddenly. This resulted in water absorption by the samples and ultimately expansion. This malfunction was repaired the next day and the data stabilized again.

4.1.4 Cement paste flexural and compressive strength

Applying shrinkage reducing agents in cement or concrete preferably should not impact the strength of the hardened cement and concrete. Therefore, cement paste compressive and flexural strength test have been performed. The same mix designs have been used as in the previous tests.

Table 4.2 Cement paste strength mixtures

Mixture	w% of cement SRA	Cement [g]	SRA [ml]	Deionized water [ml]	Total Fluid [ml]
ref	0	5000	0	2400	2400
052	0,52	5000	26	2374	2400
156	1,56	5000	78	2296	2400
261	2,61	5000	130,5	2165,5	2400

To investigate the strength development measurements have been performed after 1, 3, 7, 14 and 28 days. For each measurement 3 prisms were cast, so for each mixture a total of 15 prisms were cast.

The samples were tested in a hydraulic press and were then placed on a 3-point bending mount. The mount has a span of 10 cm, and the pressure point is in the middle. Due to the test, the prisms were broken into two pieces at approximately the middle, these two pieces were then used for the compressive tests. This way each flexural strength specimen gave 2 samples for compressive strength. In Figure 4.10 the cement paste flexural strength is plotted. The strength development between the mixtures was similar. Due to the fact that the rate of hydration is lower for higher concentrations of SRA it was expected that the strength would reduce for higher SRA content. This was observed for the 156 and 261 mixtures. The flexural strength of these two mixtures were lower at every moment in time with respect to the reference mixture. Mixture 261 was also weaker than mixture 156. The 14-day strength of 261 and 156 were really close together with strengths of 6.64 MPa and 6.70 MPa for 156 and 261, respectively. But the 156 mixture increased more in strength towards the 28 day mark. The flexural strength of the 052 mixture was relatively unexpected, because this mixture showed a lower rate of hydration with respect to the reference mixture. This also resulted in a lower degree of hydration. Therefore, it was expected that the flexural strength would be lower than that of the reference sample. The strength increase was quite significant with a minimum of 0.508 MPa at 3 days and a maximum of 1.659 MPa after 28 days of hydration. This is a flexural strength increase of 8% and 19% after 3 and 28 days, respectively. This higher strength indicates why the 052 mixture showed lower shrinkage than the 156 mixture. When the paste is stronger the resistance against shrinkage deformation is also higher, therefore the obtained

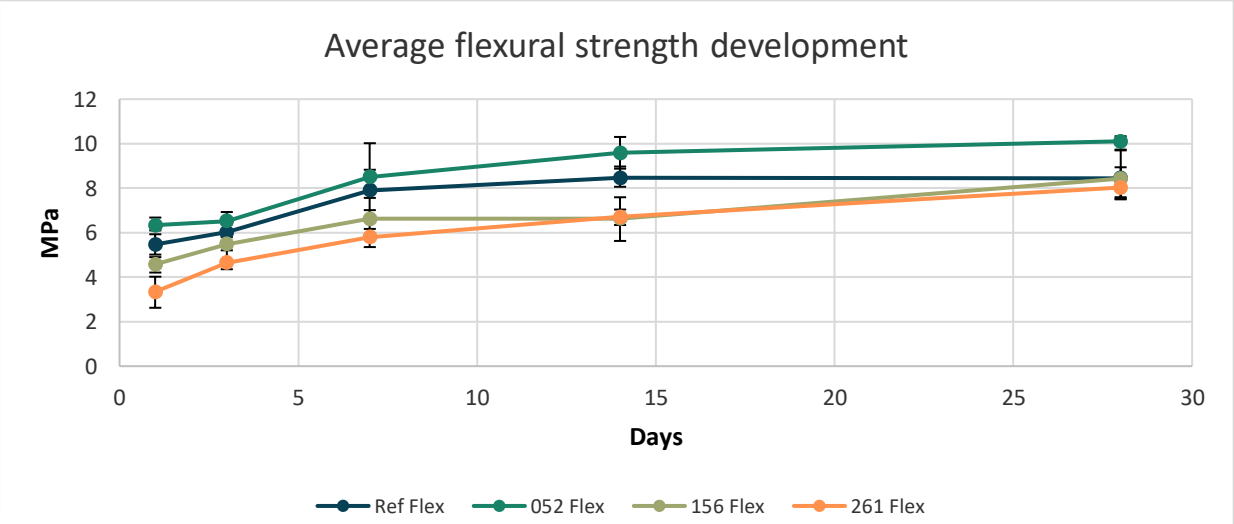

Figure 4.10 Average flexural strength development in MPa. Ref Flex=Blue, 0 w% SRA; 052 Flex=Dark green, 0.52 w% SRA; 156 Flex=Light green, 1.56 w% SRA; 261 Flex=Orange, 2.61 w% SRA.

shrinkage can in fact be lower than the shrinkage of the 156 mixture. Combining the calorimetry results with the shrinkage and weight loss results, however, does not explain why the 052 is stronger in both flexural and compressive strength than the reference sample. To find an explanation of the higher strength of the 052 mixture, the porosity of the hardened cement paste was tested.

As mentioned before, each flexural test sample was broken into two compressive test samples. These samples were placed under the press with the casting side faced sideways. This way the smooth left and right side of the prisms are in contact with the pressing plates of the press. This is done to obtain a homogenous stress across the entire cross section of 40x40 mm. The compressive tests were performed on the same days as the flexural strength test so after 1, 3, 7, 14 and 28 days. The press started measuring at 2 kN and it increased the force at a rate of 0.05 kN/s. In Figure 4.11 the average compressive strength is plotted for each mixture. The strength developments were similar for the different mixtures. It was again observed that the compressive strength of mixtures 156 and 261 were as expected with respect to the reference mixture. Here it was concluded as well that the compressive strength of the 052 mixture was consistently higher than the reference sample.

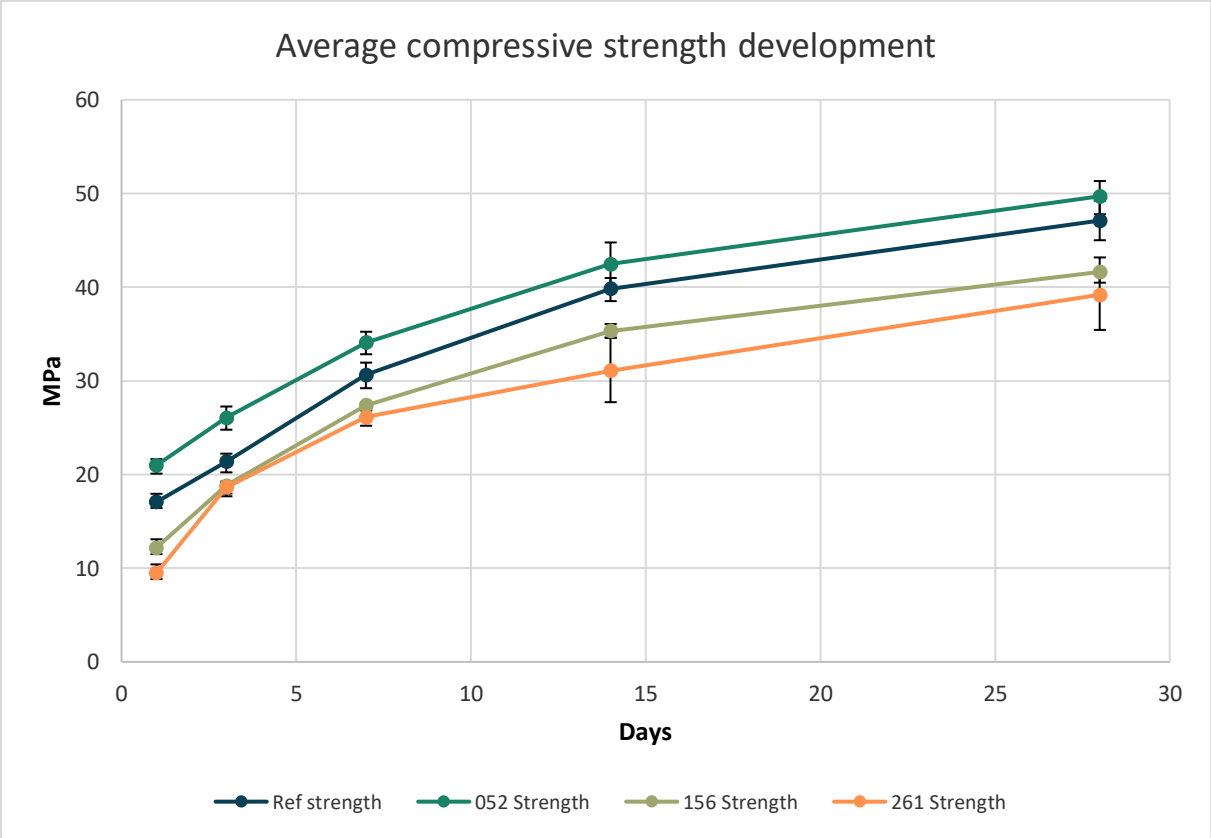

Figure 4.11 Average compressive strength in MPa. Ref strength=Blue, 0 w% SRA; 052 strength=Dark green, 0.52 w% SRA; 156 strength=Light green, 1.56 w% SRA; 261 strength=Orange, 2.61 w% SRA.

4.1.5 Mercury intrusion porosimetry

To be able to link the compressive strength, shrinkage values and weight loss, the porosity and pore size distribution were tested. A higher porosity normally results in a lower strength of the concrete. The decreased paste strength for SRA concentrations of 1.56 w% and 2.61 w% resulted in the expectation that the porosity would increase for increasing shrinkage reducing agent. In Figure 4.12 the results can be observed, the porosity increased with increasing SRA concentrations. Mercury intrusion porosimetry tests have good reproducibility therefore, it was decided to perform one measurement per sample after 1, 7 and 28 days of hydration.

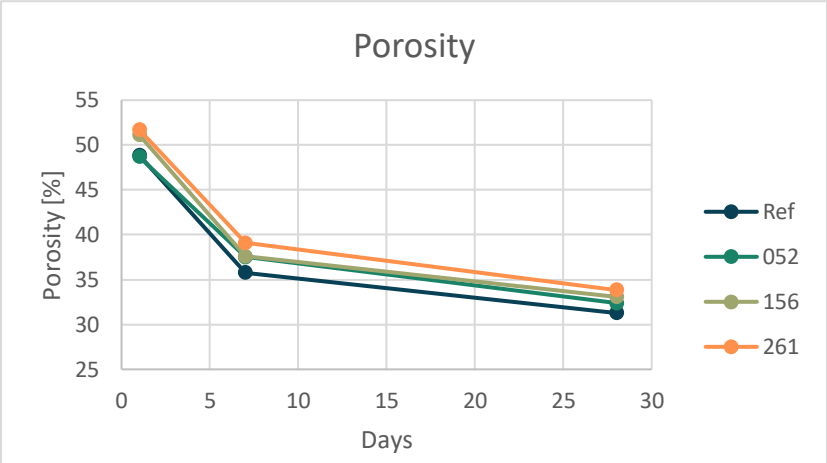

Figure 4.12 Overall porosity in %. Ref=Blue, 0 w% SRA; 052=Dark green, 0.5 2w% SRA; 156=Light green, 1.56 w% SRA; 261=Orange, 2.61 w% SRA.

Table 4.3 overal porosity

	Porosity 1 day [%]	Porosity 7 day [%]	Porosity 28 day [%]
ref	48,86	35,77	31,28
52	48,68	37,53	32,39
156	51,12	37,60	33,08
261	51,70	39,07	33,83

The increasing porosity explained why the strength of the paste and concrete samples was lower with higher SRA concentrations. However, it did not explain why mixture 052 had higher flexural and compressive strength than the reference mixture. The porosity is also very important in understanding the shrinkage behaviour of the samples. In this case the pore size distribution was most important. Larger pores result in easier and faster evaporation of water and therefore more weight loss over time. But larger pores also reduce the amount of capillary tension because the radius of the water meniscus is larger. This capillary tension, or the pressure differential between the liquid and gas interface, can be described with the equation below which is based on the Laplace equation.

$$\Delta p = \frac{2\gamma \cos\theta}{r}, \qquad \text{Equation: 6}$$

where γ is the surface tension of the capillary water, θ is the contact angle on the soli-liquid interface and r is capillary pore diameter. The pore diameter was calculated at every measuring step with the Washburn equation.

$$D = \frac{-4\gamma_m \cos\theta}{P}, \qquad \text{Equation: 7}$$

where D is the pore diameter, γ_m is the surface tension of mercury, θ the contact angle and P is the induced pressure applied by the porosimeter. With this equation the pore size distribution was obtained. In Figure 4.13 the pore size distribution per mixture is shown after 1, 7 and 28 degrees of hydration. This way the pore size development was investigated.

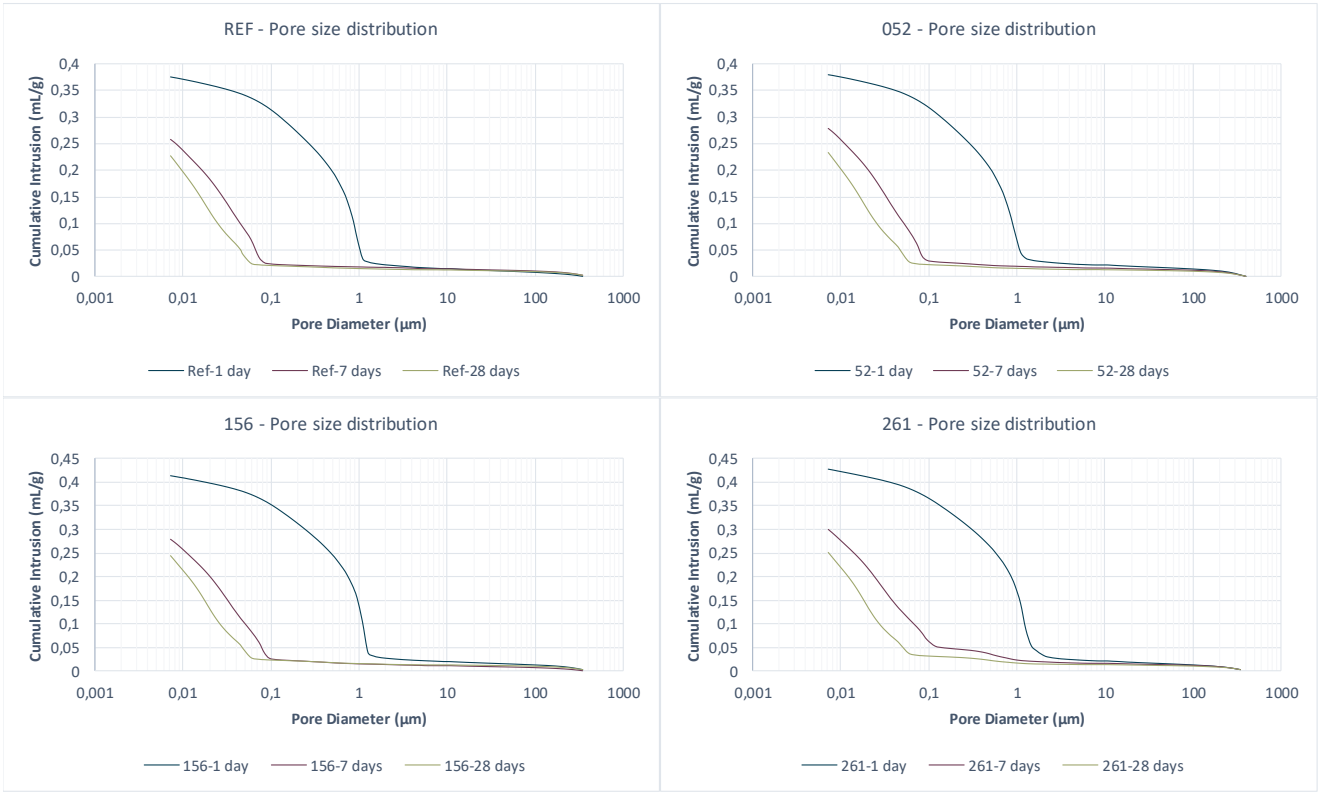

Figure 4.13 Pore size distributions per mixture. Blue=1 day porosity; Red=7 days porosity; Green=28 days porosity

To be able to compare mixtures the pore size distribution after 1, 7 and 28 days of hydration of all mixtures were plotted in one graph and shown in Figure 4.14. For every measurement, the pore volume of pores smaller than 1µm was larger for increasing SRA. The difference becomes less pronounced for longer hydration periods. After 1 day of hydration the differences were largest. However, the Ref and 052 samples were similar in pore size distribution.

Samples 156 and 261 showed a large increase in pores smaller than 1 µm. This was observed in the overall porosity values as well. After 7 days of hydration 052 and 156 were very similar and had more pores smaller than 1 µm with respect to the reference sample. The most interesting mixture was 261. This sample had more pores smaller than 1 µm than the other samples but this increase in pores was most pronounced for pores of 0.1-1 µm after 7 days of hydration. Although not as extensive, this was also the case after 28 days of hydration.

Figure 4.14 Comparison of pore size distributions. Top=Day 1 porosity per mixture; Middle=Day 7 porosity per mixture; Bottom=Day 28 porosity per mixture.

4.2) Test results Part II: Concrete

The results of the experiments on the concrete samples are given below.

4.2.1 Concrete shrinkage measurements

Like the cement paste shrinkage test the samples were wrapped and therefore no water could evaporate. The weight loss shown in Figure 4.21 confirmed that no weight and therefore no water was lost in the first 7 days of hydration. During the first seven days it could be concluded that the shrinkage measured was autogenous shrinkage. After seven days the prisms were exposed to the air to dry, from this point onward the drying shrinkage was measured. The total shrinkage is plotted against the time since casting in Figures 4.15-4.18. Per mixture three prisms were tested, these prisms and their average were plotted in their own figure. To compare them more easily the averages were plotted together in Figure 4.19.

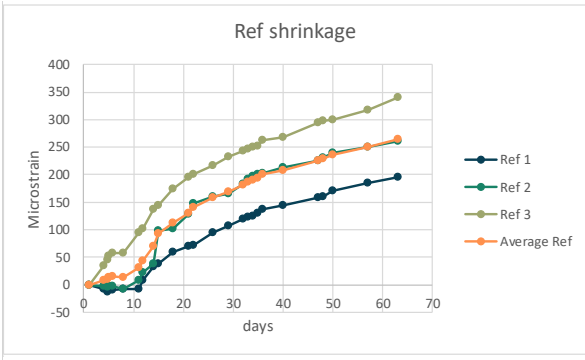

Figure 4.15 Ref autogenous and drying shrinkage; 0 w% SRA

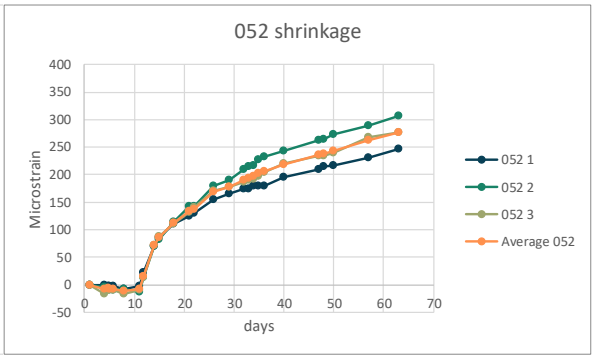

Figure 4.16 052 autogenous and drying shrinkage; 0.52 w% SRA

When the graphs that depict the shrinkage per mixture were investigated it was observed that the accuracy of the prisms per mixture is very good. Only for the reference samples the shrinkage curves were not as close as for the other mixtures. However, the curves did follow the same trend in shrinkage behaviour. During the autogenous shrinkage part, none of the samples showed shrinkage except prism Ref 3. All the other prisms showed slight expansion, increasing with increasing SRA content. After the prisms were exposed to the air all the prisms started to shrink. The lower the SRA content the more gradually but also the more extensive the shrinkage. For the 261 mixture and even for the 156 mixture it was observed that in the first two days after unpacking the prisms shrank quite suddenly, but the shrinkage graph flattened rapidly afterwards.

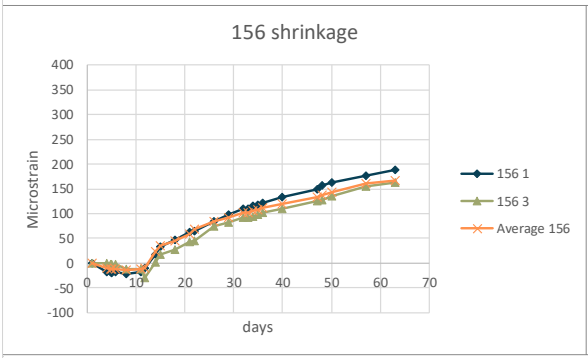

Figure 4.17 156 autogenous and drying shrinkage; 1.56 w% SRA

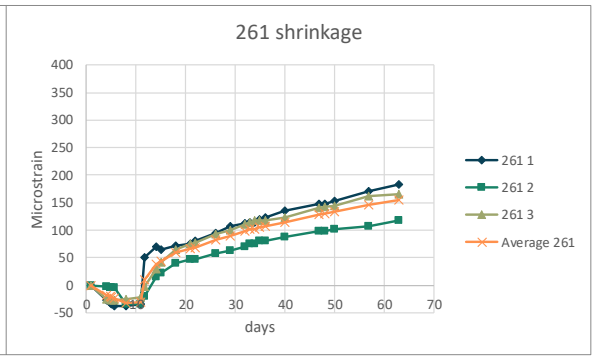

Figure 4.18 261 autogenous and drying shrinkage; 2.61 w% SRA

In Figure 4.19 the average shrinkage is shown of the different mixtures. The figure indicates that the average shrinkage of the 156 and 261 mixtures were very close together and show approximately 47% less total shrinkage when compared to the reference mixture after 28 days of hydration. The average shrinkage of the 052 mixture was quite surprising because it was expected to have less shrinkage than the reference mixtures. However, it showed approximately 5% more total shrinkage after 28 days of hydration. This is consistent with the observation that the 052 mixture lost much more weight with respect to the other mixtures. This can be observed in the weight loss graphs in Figure 4.21. Mixtures 156 and 261 lost similar amounts of moisture, approximately 6% less with respect to the reference mixture. The 052 mixture however lost 19% more moisture with respect to reference mixture. Drying shrinkage increases with increased loss of moisture so from this it was expected to find a higher shrinkage value for the 052 mixture and less shrinkage for the 156 and 261 mixtures with respect to the reference mixture. A higher shrinkage strain for mixture 052 could possibly be explained with the porosity results. These results showed an increase in porosity for higher SRA content. The difference in porosity was mainly because the number of small fine pores between 8 nm-1 µm increased for higher SRA content. Of course, there is the balance of higher porosity and lower surface tension. If the SRA resulted in a higher porosity of the hardened cement paste the concrete will lose moisture more easily which results in higher drying shrinkage. Conversely, the SRA actively lowers the surface tension of the water in the samples, which lowers the capillary tension resulting in lower shrinkage. The increased porosity cancels a part of the lower capillary tension. Therefore, it is possible that applying 0.52 weight percentage of cement fraction of SRA is too low to be effective.

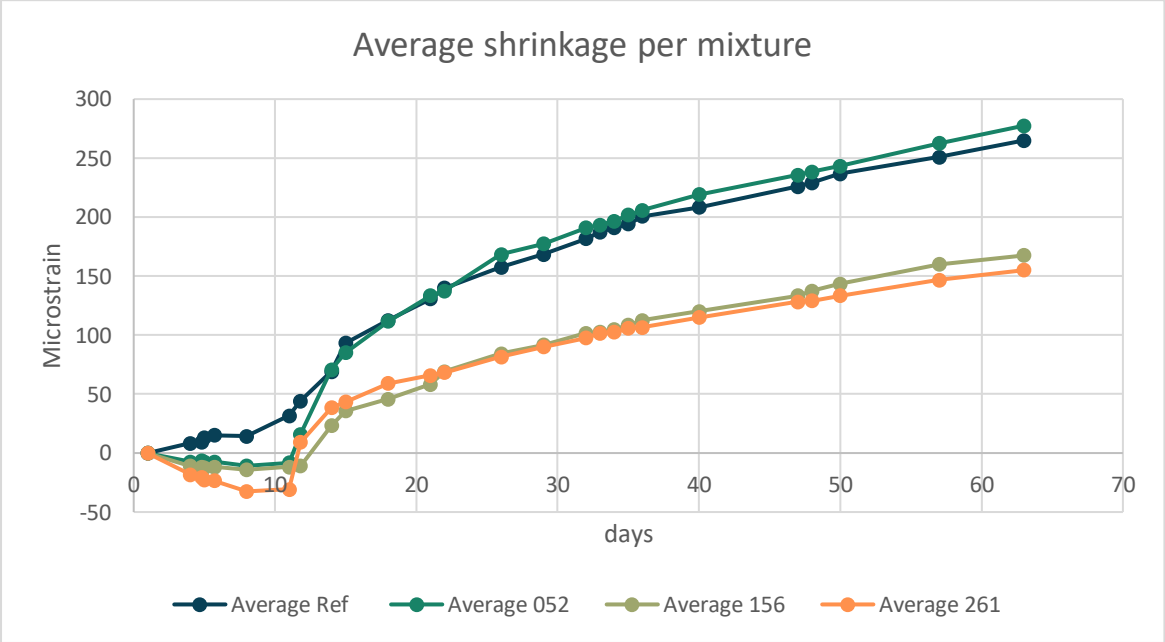

Figure 4.19 Average autogenous + drying shrinkage per mixture. First 7 days is autogenous shrinkage. After 7 days samples are exposed to drying and drying shrinkage is measured. Blue=Reference, 0 w% SRA; Dark green=052, 0.52 w% SRA; Light green=156, 1.56 w% SRA; Orange=261, 2.61 w% SRA.

In Figure 4.20 the autogenous shrinkage was removed from the graph and only the drying shrinkage is shown. In Figure 4.20 the effect of different SRA concentrations on the drying shrinkage is clear. The differences in drying shrinkage between the reference mixture and mixture 052 increased, as well as the difference between mixtures 156 and 261. It was observed that 2.61 w% SRA decreased drying shrinkage the most by 44% after 51 days of hydration. Mixture 156 performed second best with a drying shrinkage reduction of 19%. Drying shrinkage of mixture 052 increased by 18% with respect to the reference sample.

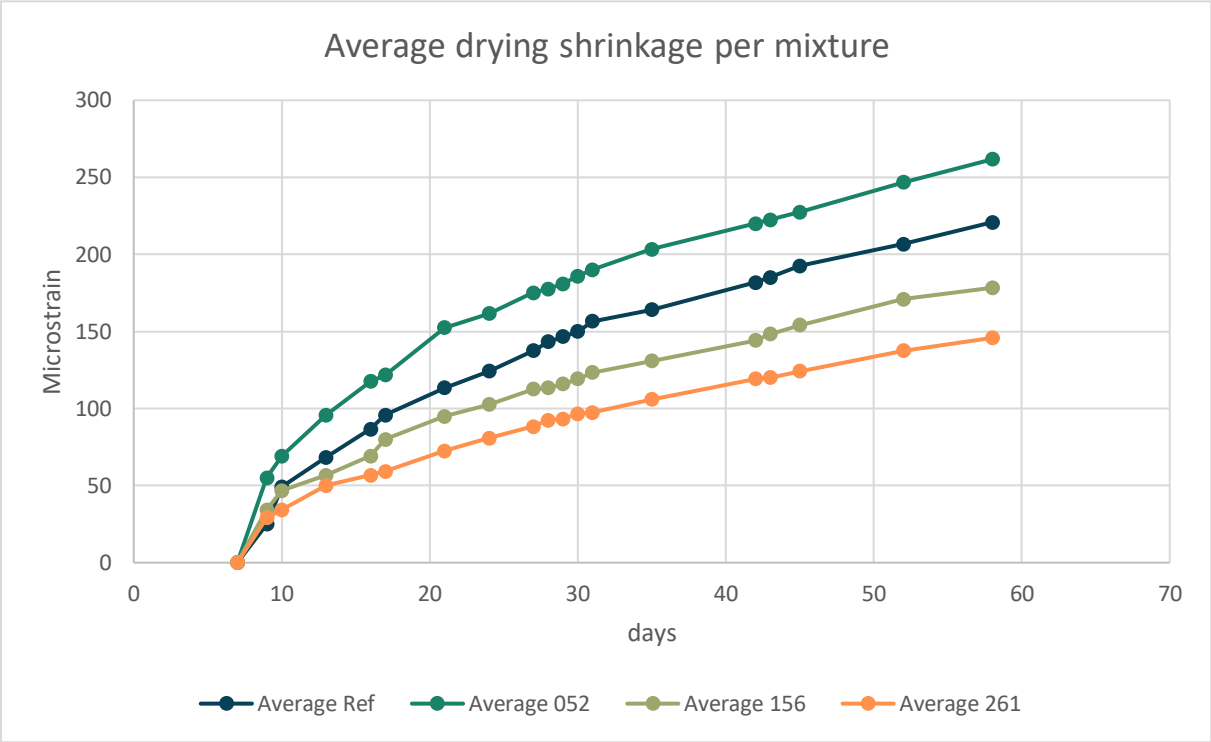

Figure 4.20 Average drying shrinkage per mixture from moment of unwrapping (day 7). Blue=Reference, 0 w% SRA; Dark green=052, 0.52 w% SRA; Light green=156, 1.56 w% SRA; Orange=261, 2.61 w% SRA.

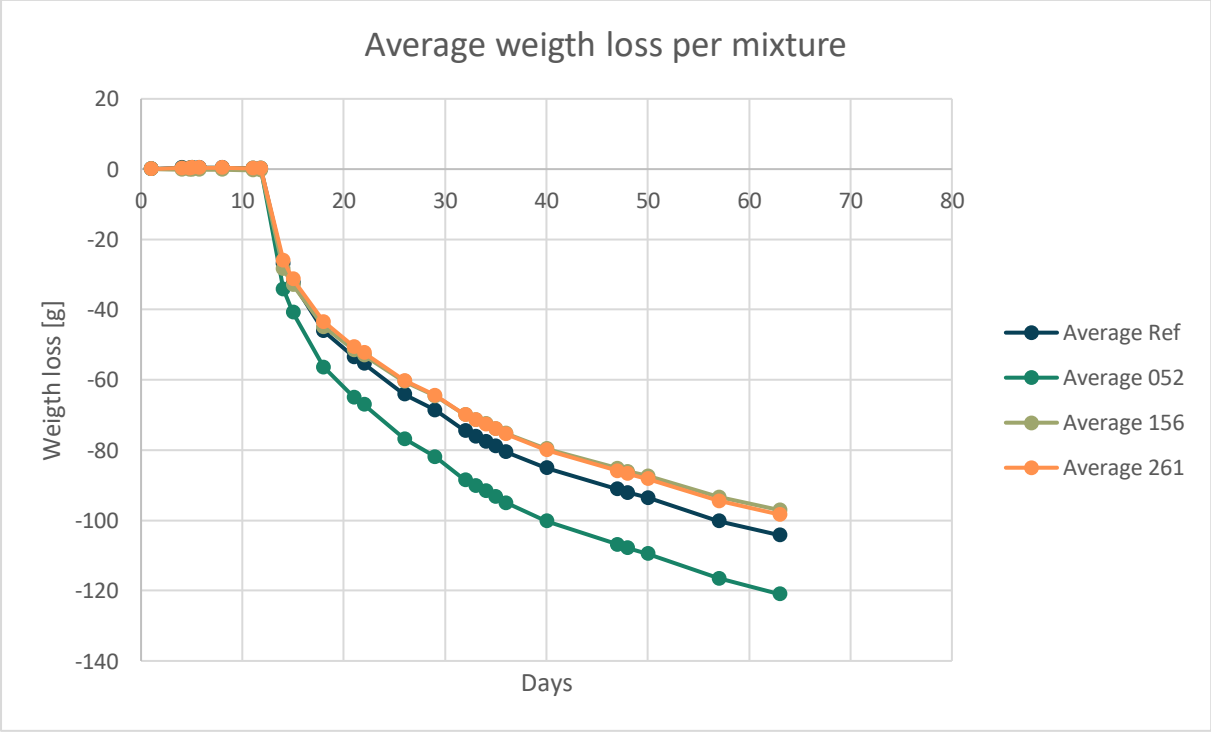

Figure 4.21 Weight loss per beam. First 7 days no weight loss was measured due to plastic foil. After 7 days samples were unwrapped and started drying. Mixtures Ref (0 w% SRA), 156 (1.56 w% SRA) and 261 (2.61 w% SRA) are very similar. Mixture 052 (0.52 w% SRA) loses more weight with respect to the other mixtures.

4.2.2 Cube compressive strength

In this section the compressive strength development is discussed. For each mixture 9 cubes of 15x15x15 cm have been cast using the same four mix designs. The cube compressive strength was measured after 1, 7 and 28 days of hydration. This resulted in 3 cubes per test moment per mixture. In Figure 4.22 the compressive strengths per mixture have been plotted. In these graphs it was observed that the strength development is very similar for each mixture and the deviations per mixture are small.

With respect to the theory it was expected that the compressive strength would reduce with

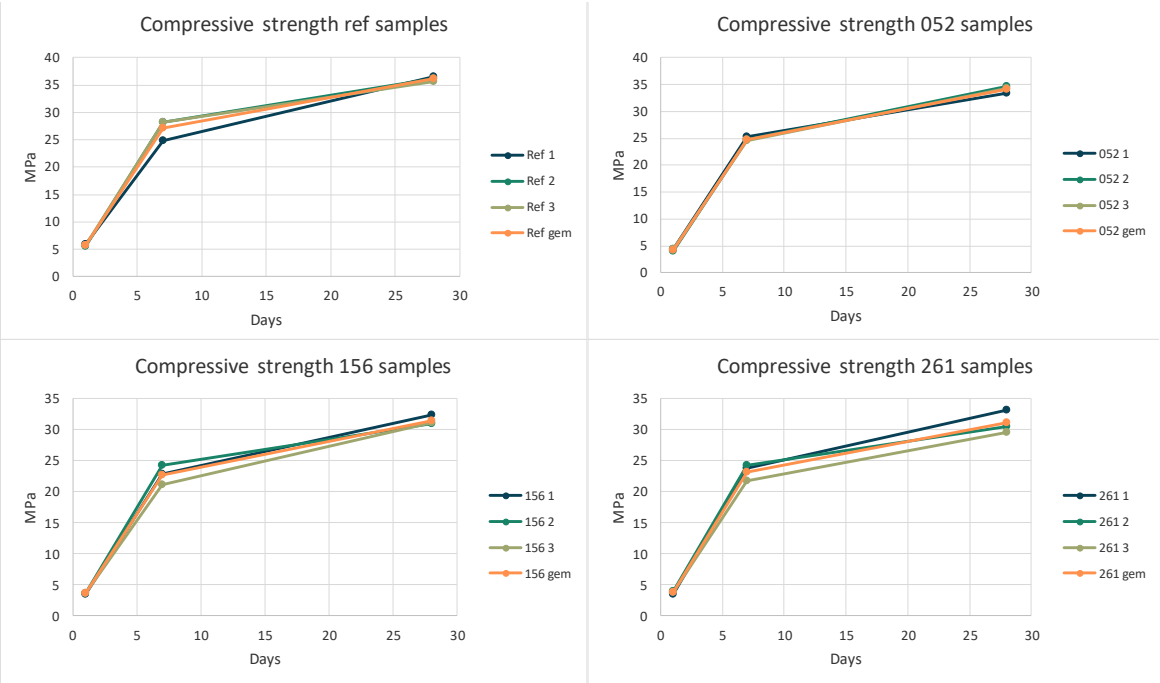

Figure 4.22 Concrete cube compressive stresses per mixture. Ref= 0 w% SRA; 052= 0.52 w% SRA; 156= 1.56 w% SRA; 261= 2.61 w% SRA.

increasing SRA content, the measured average stresses confirmed this (Figure 4.23). After 28 days of hydration the compressive stress was 36.08, 34.06, 31.5 and 31.07 MPa for Ref, 052, 156, and 261, respectively. It was observed that the 156 and 261 mixtures had very similar compressive strengths. The 261 actually had a slightly higher compressive strength after 1 and 7 days, 3.8% and 2.2% respectively. These differences are small when compared with the 34.3% diffrence between the reference and 261 mixture. Mixture 052 showed expected behaviour, by having compressive strengths that are always between the strengths of the reference and the 156 mixture. This was interesting to see because the compressive strength test on the cement paste showed the highest compressive stress for the 052 mixture. This can be explained by the shrinkage measurements and porosity measurements. The cement paste of 052 showed a surprisingly low drying shrinkage, even less than the 156 mixture while loosing slightly more moisture. Less shrinkage was most likely due to the fact of the higher stength development. Stronger cement paste has better resistance against shrinkage. The porosity of the 052 mixture showed a lower value than the other mixtures with SRA after one day of hydration. The denser structure explained the higher compressive strength, it does not however explain why more moisture is lost. It is to be expected that a lower porosity results in less evaporation of water. Water evaporates more easily from larger pores, but the pore size distribution did not show an increase in large pores. The compressive strength of the 052 concrete mixture is completely as expected even though it shrinks more than the reference samples due more loss of water. The condition for each prism was the same, the hydration rate was lower, porosity increased, shrinkage

values were higher than the reference samples, more water evaporated but compressive strength values were normal. These experimental results of mixture 052 so far are unpredictable and contradict eachother. In chapter 5 this will be discussed to a larger extend.

Mixtures 156 and 261 showed very similar behaviour with respect to the strength development, but also the total shrinkage values. In both experiments the graphs were very similar and comparable. Even the cement paste compressive strength of these mixtures showed similarity. The main difference was that mixture 156 had higher drying shrinkage on the cement paste and concrete level, it also showed more weight loss, as expected. The interesting part was that the cement paste of sample 261 showed less shrinkage, but also lower flexural and compressive strength with respect to mixture 156. One could say that increased shrinkage reduction came with a strength reduction. This is however, not observed in the concrete tests. Sample 261 showed less autogenous shrinkage and drying shrinkage when compared to mixture 156. Therefore, 261 performs slightly better than mixture 156 if the shrinkage is considered. This slight improvement of shrinkage behaviour is actually not countered by a strength decrease.

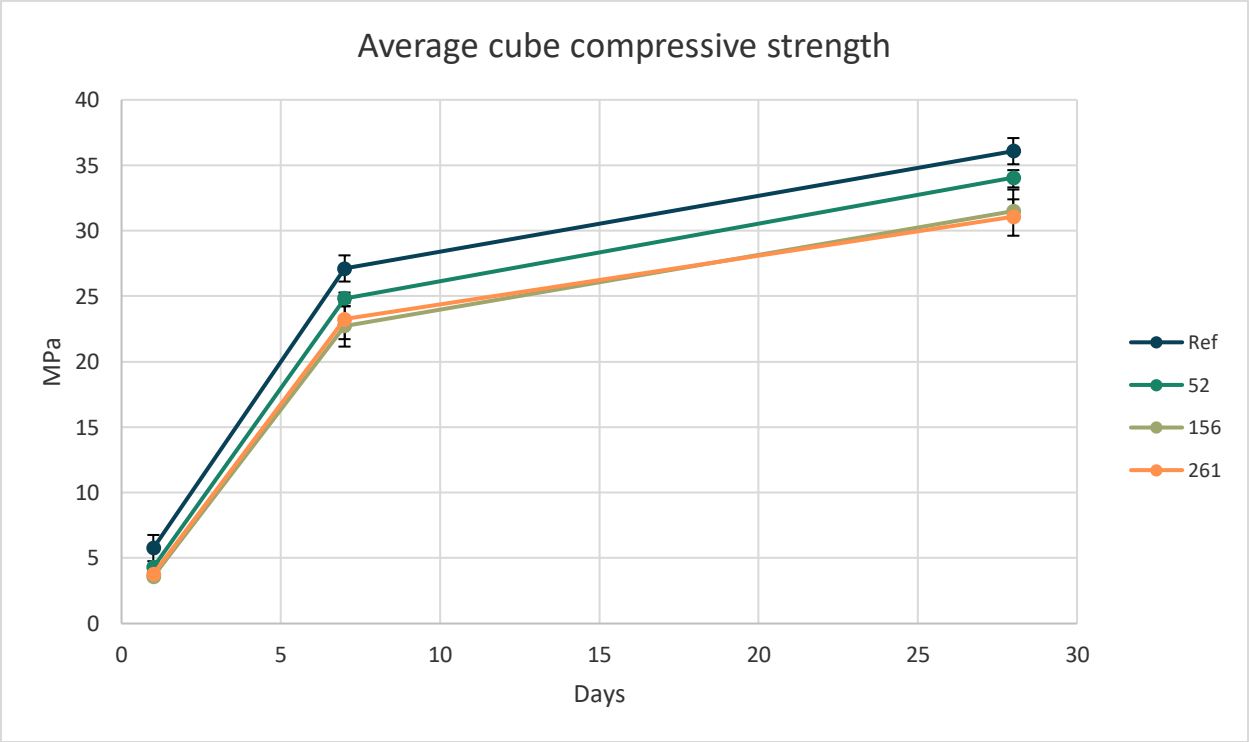

Figure 4.23 Average cube compressive strength per mixture. Ref=Blue, 0 w% SRA; 052=Dark green, 0.52 w% SRA; 156=Light green, 1.56 w% SRA; 261=Orange, 2.61 w% SRA.

4.2.3 Young's modulus

When the cube compressive strength and the shrinkage was measured the modulus of elasticity was also investigated. Otherwise the cube compressive strength and shrinkage values cannot be evaluated properly. The elastic modulus as well as the Poison's ratio were calculated. The LVDTs measured an absolute length change in mm and the applied force was in kilonewton. The area of the prism was used to calculate the stress, and the distance between mounts was used to calculate the strain. The elastic modulus was calculated using the following formula:

$$E = \frac{\sigma}{\varepsilon}, \qquad \text{Equation: 8}$$

where E is the elastic modulus in Pa, σ is the compressive stress in Pa and ε is the strain. The averages of the four vertical LVDTs were used to calculate the elastic modulus. The averages are shown in Figure 4.24.

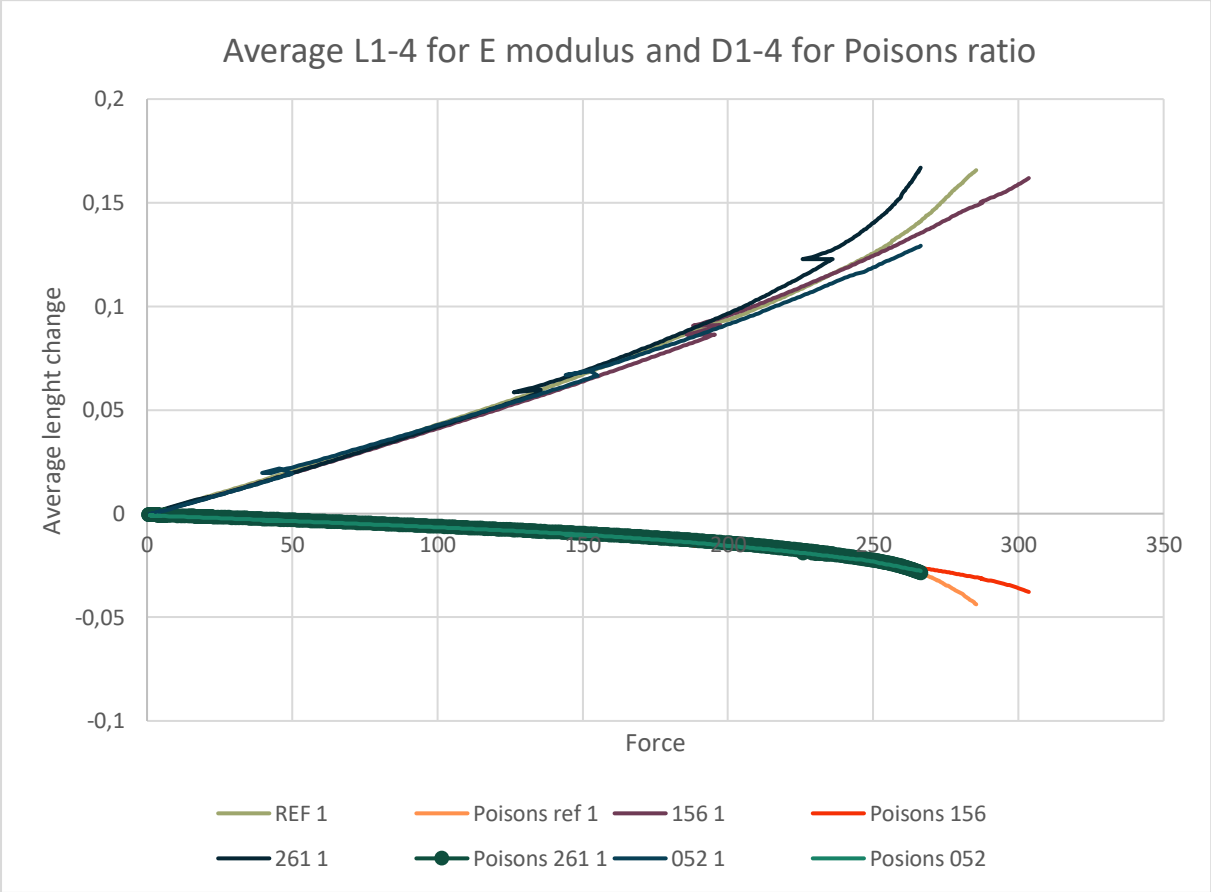

Figure 4.24 Average values L1-4 per mixture; Average values D1-4 per mixture

The calculated elastic moduli are shown in Table 4.4.

Table 4.4 Elastic modulus

Prism	E-modulus [GPa]
Ref 1	36,09
052 1	26,39
156 1	41,71
261 1	33,60

The poisons ratio is the ratio between lateral and longitudinal strain. It can be calculated as follows:

$$v = -(\frac{\varepsilon_{xx}}{\varepsilon_{yy}}), \qquad \text{Equation: 9}$$

Where v is the poisons ratio, ε_{xx} is the horizontal strain and ε_{yy} is the vertical strain. The values for each mixture are given in Table 4.5. The poison's ratio is for concrete is normally between 0.15 and 0.20. All the found values are in this range so they can be considered accurate.

Table 4.5 Poisons ratio

	Poisons ratio
Ref	0,153
52	0,168
156	0,179
261	0,151

5) Summary of results

In this research the mechanism of drying shrinkage reduction of SRA was investigated alongside its influences on the hydration process and mechanical properties. By performing experiments, results were obtained to gain insight in these influences of applying SRA in concrete, presented in chapter 4. In this chapter these results are summarised and the connection to basic principles of shrinkage reducing agents is made. The effects of applying SRA are explained using the Kelvin (Equation: 3) and the reduction of surface tension as starting point.

The investigated properties are discussed in the same order as the previous chapters (see summary below). The division into cement paste and concrete experiment is also maintained. Each division is started with a graphical overview of the results and followed by a summary and explanation per property.

1 - Surface tension of mixing water,
2 - Rate of hydration
3 - Degree of hydration
4 - Porosity
5 - Pore size distribution
6 - Compressive strength
7 - Flexural strength
8 - Drying shrinkage
9 - Weight loss
10 - Elastic modulus

5.1) Summary of cement paste results

Figure 5.1 Results comparison cement paste. Percentages are with respect to the reference mixture.

5.1.1 Surface tension

Increasing the amount of Sika Control 40 reduces the average surface tension by 11-29% for 0.52, 1.56 and 2.61 percentage of weight. Increasing the concentration has diminishing returns on reducing the surface tension due to the critical micelle concentration (CMC). At this concentration, the SRA starts to aggregate in the bulk of the liquid instead of being located at the solid-liquid interface (Rosen, 2004). The SRA actively lowers the surface tension when its located on this solid-liquid interface. Therefore, surfactant molecules that formed micelles do not contribute to the surface tension reduction. It was observed in section 4.1.1 that the surface tension reduction was not linear with the SRA concentration. Apparently, there was a surplus of SRA for concentrations of 1.56 w% and 2.61 w% and the SRA started to form micelles in the bulk of the water. Therefore, the effectivity of the SRA reduced with respect to the surface tension reduction.

5.1.2 Rate of hydration

The rate of hydration is lower for increasing SRA content. The initial hydration peak is 4%, 17% and 28% later than the reference for 052, 156 and 261 respectively. The second hydration peak corresponding to the hydration of slag is 6%, 13% and 25% later than the reference mixture. The cumulative heat is 7%, 6% and 5% lower than the reference mixture. As mentioned in section 5.1, surfactant molecules are primarily located at the solid-liquid interface in concrete (Rosen, 2004). The surfactant molecules form a layer between the water and cement, or between the water and aggregate. Rajabipour et al. (2008) observed a reduction in the dissolution rate of alkalis when SRA was added. The layer of surfactant hinders the contact of water with unhydrated cement thereby, slowing down the hydration process. When more SRA is applied, the hydration rate reduction is more pronounced. The reduction in cumulative heat can confirm this. The total cumulative heat after 7 days was lower when SRA was applied compared to the reference. The cumulative heat is a measure of degree of hydration (Neville, 1995; Reinhardt, 1998). After 7 days the degree of hydration is lower for mixtures with SRA, meaning that less cement particles could react with water in the presence of SRA.

5.1.3 Porosity

After 1 day of hydration the overall porosity increased by 0%, 5% and 6% for 052, 156 and 261 respectively. The porosity differences changed after 7 days of hydration to 5%, 5% and 9% for 052, 156 and 261 respectively. After 28 days porosity increases of 4%, 6% and 8% is observed. The pore size distribution showed that the volume of gel pores increased for increasing SRA content after 1, 7 and 28 days of hydration. Porosity in cement paste depends on the degree of hydration and the temperature. A lower degree of hydration and higher temperature during hydration results in a higher porosity (Neville, 1995; Reinhardt, 1998). Calorimetry results showed a decrease in degree of hydration, this was discussed in section 4.1.2 and section 5.2. This lower degree of hydration results in higher porosity. The temperature during cement hydration was 20 ^{o}C for all mixtures. The decrease in total cumulative heat for mixtures with SRA would result a slightly lower temperature of the hydrating cement paste. This difference, however, is small. The porosity of samples with SRA increased due to the reduction of degree of hydration. This result is more pronounced for increasing SRA concentrations.

5.1.4 Cement paste shrinkage

The cement paste shrinkage after 28 days of hydration is depicted (Figure 5.1). Shrinkage is reduced by 5%, 9% and 15% for mixtures 156, 052 and 261, respectively. Interesting to observe here is that 156 shrinks more than 052. In advance it was expected to be reversed based on the Kelvin equation. Higher SRA concentrations resulted in lower surface tension and should ultimately result in lower capillary tension and shrinkage. However, this result can be explained based on the other test results. The compressive and flexural strength of the 052 cement paste is at least 20% higher at every moment with respect to 156. The porosity of 156 is higher than 052 as well, especially the number of pores <1 µm are increased. According to the Laplace law (Equation: 1), capillary tensile stress is higher in smaller pores, resulting in a higher drying shrinkage. The difference in strength and increase in number of small pores outweighed the increased amount of SRA with respect to the drying shrinkage. Sample 261 has lower compressive strength and higher porosity than samples 052 and 156, it has the lowest drying shrinkage of all mixtures. For mixture 261 the number of small pores was higher than for mixture 156 and strength was lower. However, shrinkage reduction was higher. In the samples with SRA concentration of 2.61 w% the reduction of surface tension resulted in a higher decrease in capillary tension than the increased number of pores increased the capillary tension. Resulting in drying shrinkage reduction.

5.1.5 Cement paste weight loss

A weight loss reduction of 5%, 9% and 15% is observed for mixtures 052, 156 and 261, respectively. Evaporation of water, weight loss, depends mainly on environmental conditions and microstructure of cement paste. Environmental conditions were similar for all samples thus it was discarded to have influence on the weight loss. The microstructure, especially the pore size distribution, is an important factor for evaporation of water. Higher overall porosity normally results in easier evaporation of water. However, water evaporates more easily from larger pores than from small pores. Applying SRA resulted in a higher overall porosity for increased SRA concentrations. In section 4.1.5 it was observed that the number of pores for all pore sizes increased for increasing SRA content. Therefore, evaporation of water should be higher for increasing SRA content. However, the results showed a decrease in evaporation of water. Applying an SRA reduced the surface tension of water and acted like a wetting agent. Wetting agents decrease cohesive forces in water and increase adhesive forces of water and cement paste (Rosen, 2004). The water in the pores will spread out more and adhere to the cement paste making the evaporation of water more difficult. This is more pronounced for higher SRA concentrations.

5.1.6 Cement paste flexural strength

With respect to the reference sample, sample 052 shows an increased flexural strength of 16%, 8% and 20% after 1, 7 and 28 days, respectively. Sample 156 is 16%, 16% and 0% weaker than the reference after 1, 7 and 28 of hydration, respectively. Sample 261 is the weakest in flexural strength with values after 1, 7 and 28 days of hydration which are 39%, 27% and 5% lower than the reference mixture. Cement paste strength is strongly dependant on mix design, rate of hydration and porosity (Neville, 1995; Reinhardt, 1998). Mix design was constant for all mixtures except for SRA concentrations. The SRA decreased the rate of hydration and therefore the strength development was reduced as well. And the SRA increased the porosity of the hardened cement paste resulting in lower flexural strength. The increase in flexural strength of mixture 052 was unexpected based on the previous results. Due to the increase in porosity and lower rate of hydration it was expected that mixture 052 would be weaker than the reference mixture. The increase in flexural strength of mixture 052 could not be fully explained based on the available results.

5.1.7 Cement paste compressive strength

With respect to the reference sample 052 shows an increased compressive strength of 23%, 11% and 5% after 1, 7 and 28 days, respectively. Sample 156 is 29%, 11% and 12% weaker than the reference after 1, 7 and 28 of hydration, respectively. Sample 261 is the weakest in compressive strength with value after 1, 7 and 28 days of hydration which are 44%, 15% and 17% lower than the reference mixture. Applying the SRA resulted in shrinkage reduction but also caused a decrease in both flexural and compressive strength of cement paste. A similar explanation is applicable here as in section 5.6. Applying SRA decreased the rate of hydration and increased the porosity of the cement paste resulting in lower compressive strength. The increase in compressive strength of mixture 052 was unexpected. With respect to the reference mixture the rate of hydration of mixture 052 was slower and porosity was higher. Therefore, expectations were that mixture 052 was weaker in compressive strength. Similar to the flexural strength results no complete explanation is available for the increase in compressive strength of mixture 052.

5.2) Summary of concrete results

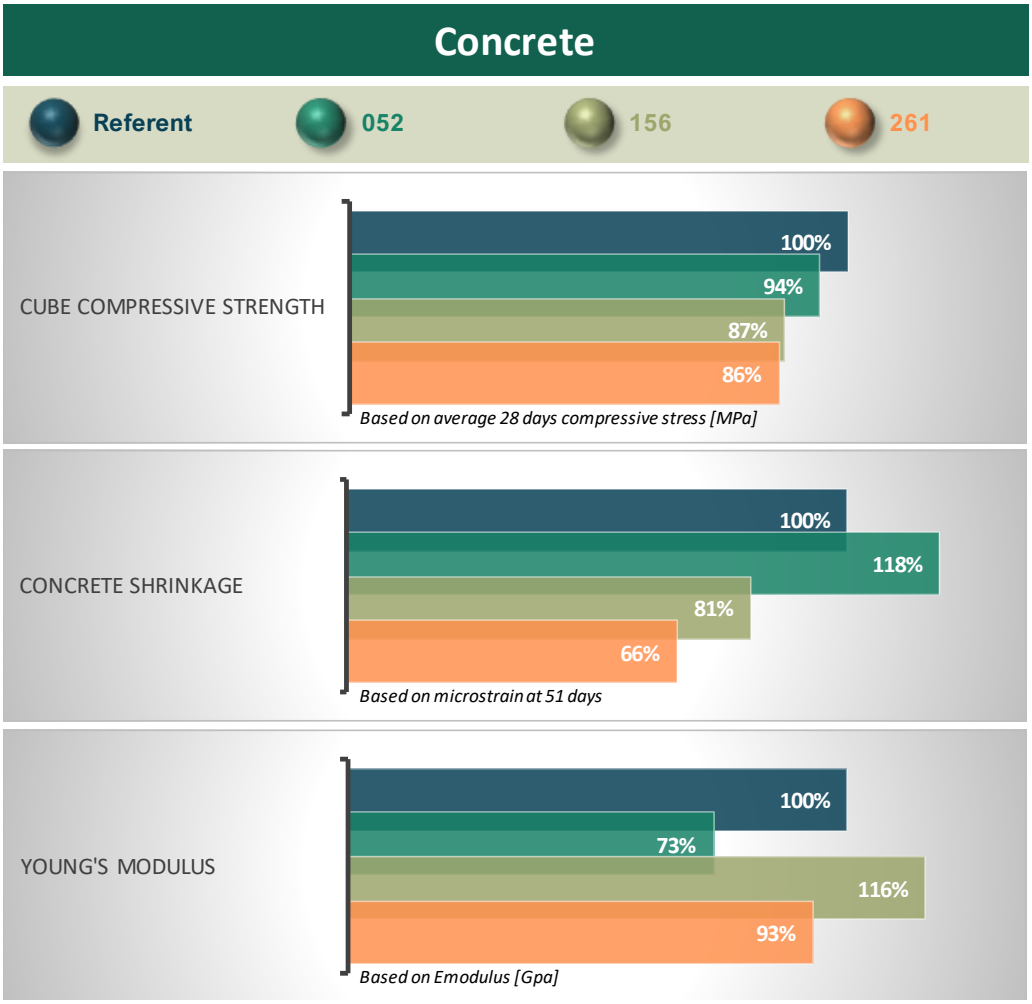

Figure 5.2 Results comparison concrete. Percentages are with respect to the reference mixture.

5.2.1 Concrete cube compressive strength

The compressive strength decreases with increasing SRA content. 28 days cube compressive strength decreases by 6%, 13% and 14% for mixtures 052, 156 and 261, respectively. As explained in section 5.6 the decrease in strength can be explained by the increase in overall porosity and the lower rate of hydration. Strength development is slower when the hydration rate is lower and an increase in porosity results in a less dense structure. Therefore, it was expected that a lower compressive strength was obtained. The differences in compressive strength after 1, 7 and 28 do not change much. Therefore, the compressive strength of the concrete appears not to be limited by the hydration rate only. Otherwise the difference would decrease over time. The compressive strength for mixture 052 was as expected based on the expected results and theory. Mixture 052 was weaker than the reference mixture and stronger than mixture 156 and 261. However, compared to the strength of the cement paste of mixture 052 these results are strange. Cement paste is the binder for the aggregates in concrete and the strength of the paste greatly determines the strength of concrete. Based on the cement paste compressive strength results, mixture 052 should have a higher concrete compressive strength with respect to the reference mixture. During this research no clear explanation was obtained for the behaviour of mixture 052. The obtained experimental results of mixture 052 contradict each other therefore, mixture 052 is unpredictable in its behaviour.

5.2.2 Concrete drying shrinkage

For mixtures 156 and 261 the concrete drying shrinkage reduced by 36% and 48% after 28 days of hydration. After 51 days of hydration these values changed to 32% and 45%. Applying the SRA caused a decrease in loss of water from these samples and the reduction in surface tension reduced capillary tensile stresses. Even though the overall porosity of these two mixtures is higher than that of the reference mixture and the number of gel pores is slightly higher shrinkage was still reduced. Mixture 052 showed an increase in concrete drying shrinkage of 23% and 18% after 28 and 51 days of hydration. For this mixture, an increased loss of water is observed which explains higher drying shrinkage. The porosity values and pore size distribution did not show higher overall porosity nor more capillary pores with respect to the reference mixture, which would lead to more water evaporation. Applying SRA concentration of 0.52 w% of cement appears to ease water evaporation from the concrete and, therefore, cancel the reduction in capillary tension. The expected wetting agent behaviour observed in the cement paste weight loss experiments was not observed in the concrete samples of mixture 052. The higher SRA concentrations of 1.56 w% and 2.61 w% did show the expected reduction in water evaporation.

5.2.3 Elastic modulus

The elastic modulus of concrete normally is in the range of 30-50 GPa. One test[3] was performed on the four mixtures and the values are:

Table 5.1 Elastic modulus

Prism	E-modulus [GPa]
Ref 1	36,09
052 1	26,39
156 1	41,71
261 1	33,60

The obtained values are within the expected range except mixture 052. The elastic modulus of 052 is relatively low with respect to the other three mixtures. In Figure 5.2 the modulus is expressed in percentages and 052 is 27% lower than the reference. If this value is accurate, which is assumed it is, then the increased drying shrinkage of this mixture can be clarified. With lower elastic modulus, deformation like shrinkage could be easier to achieve. Therefore, a higher evaporation rate of water and a lower elastic modulus could increase the amount of drying shrinkage. The differences between the reference samples and the 156 and 261 samples are less pronounced and the difference in loss of water is lower as well. That is why the behaviour of the 052 mixture is not observed for the other samples. Due to circumstances only one sample per mixture could be tested. This sample size is small therefore, the influence of SRA on the elastic modulus cannot accurately be derived. According to Eberhardt (2010, p. 44) ‘‘There seems to be no significant change for the development of the modulus of elasticity in presence of SRAs (compressive setup)’’. Based on this statement and results obtained in section 4.2.3, it is assumed that the derived values for the Young’s modulus are accurate.

5.3) The effects of SRA

Altogether the shrinkage reducing agent has positive effects on the surface tension, weight loss and drying shrinkage for concentrations of 1.56 w% and 2.61 w% of cement. It has negative effects on rate and degree of hydration, porosity, pore size distribution, compressive and flexural strength for concentrations of 1.56 w% and 2.61 w%. The elastic modulus lacks adequate data to observe a trend, however the results are within the range of expected values for concrete for mixtures 156 and 261.

[3] Due to the covid-19 virus further tests had to be cancelled.

The elastic modulus for mixture 052 was lower than expected. Mixtures with SRA concentrations of 1.56 w% and 2.61 w% of cement showed expected behaviour and experimental results explained this behaviour. However, an SRA concentration of 0.52 w% of cement resulted in unpredictable and contradicting results.

To provide the results in a clear and comparable way, an overview was given (see also Figure 5.1 and Figure 5.2). This overview can be used to predict influences of the shrinkage reducing agents and it can be used in practice to design a concrete mix, and check if the expected properties will be achieved. In the graphical overviews (Figure 5.1 and Figure 5.2) the four mixtures are weighed against each other per test. All the test results are expressed in percentages for easier comparison and weighed against the reference sample meaning that the reference sample is put at 100%.

6) Conclusion and outlook

In this research the mechanism of shrinkage reducing agents like Sika Control 40 was investigated. Information and understanding on the mechanism of shrinkage reduction were obtained. Influences of Sika Control 40 on the hydration process and the mechanical properties were investigated and discussed. Based on previous research and the practical question about how to reduce drying shrinkage with SRAs this research question was set up:

'***What is the mechanism of shrinkage reduction for shrinkage reducing agent Sika Control 40 and what are the influences on the hydration process and development of material properties?'***

With the knowledge obtained from this research this question can be answered. The shrinkage reducing agent Sika Control 40 is a surfactant. Surfactants reduce the surface tension of water due to their molecular structure. Based on the Kelvin equation the capillary tensile stress reduces when the surface tension of water reduces. Capillary tensile stress is the driving force for drying shrinkage. The reduction of surface tension of water by the SRA ultimately reduces the drying shrinkage. Consequently, applying a shrinkage reducing agent affects the hydration process and mechanical properties. The following conclusions can be drawn from the presented results:

- The mechanism of shrinkage reducing agents is based on the reducing the surface tension of water. Following the Kelvin equation (Equation 3), capillary tensile stresses are a function of surface tension, contact angle between water and cement, relative humidity, and pore size. Adding SRAs to mixing water of concrete lowers the surface tension end therefore the capillary tensile forces. Ultimately, reducing drying shrinkage and drying shrinkage cracking.
- Sika Control 40 lowers the cement hydration rate. Surfactant molecules form a barrier between the water and unhydrated cement. This barrier lowers the dissolution rate of unhydrated cement. Lower dissolution rate results in lower pH values, slowing down hydration rate even more. Rate of hydration decreased by 4%, 17% and 25% for SRA concentrations of 0.52 w%, 1.56 w% and 2.61 w% of cement fraction, respectively.
- Adding Sika Control 40 reduced drying shrinkage in cement paste by 26%, 21% and 38% for SRA concentrations of 0.52 w%, 1.56 w% and 2.61 w% of cement fraction.
- SRA concentration of 052 w% of cement in concrete samples is not effective and increased the drying shrinkage by 18% after 51 days of drying. Higher concentrations of SRA, 1.56 w% and 2.61 w% reduced drying shrinkage by 19% and 34% respectively after 51 days drying.
- Concrete strength reduced slightly by 6%, 13%, and 14% after 28 days of hydration for SRA concentrations of 0.52 w%, 1.56 w% and 2.61 w% of cement fraction.

During this research multiple topics arose that were out of scope for this research, but interesting for further research. To investigate what the implications of this research are for the practical and scientific field, a couple of notes and ideas are shared below.

6.1) Practical implications & recommendations

Besides conducting a master thesis research, this research was started with the interest of ABT in the possibilities of Sika Control 40. As this research has given more insight into the mechanisms and the effects of this SRA, a view is given here on the practical implications of this SRA. In addition, some recommendations are given.

When applying Sika Control 40 in concrete, one should especially consider the strength reduction and the lower rate of hydration. As strength development will be slower due to the SRA, this has implications for the timing of formwork removal and the timing of applying the first load on the concrete. It could in practice mean that more time is needed for casting and hardening of concrete floors, which can increase total build time.

Meanwhile, the lower drying shrinkage strains allow for the use of less reinforcements and could reduce drying shrinkage cracking. On the construction site this means improved durability of the concrete floor and reduced material usage. When looked at drying shrinkage from a simple perspective, one could say the more SRA used the better. However, there are some considerations that should be considered. The results showed that a concentration of 0.52 w% does not result in concrete drying shrinkage reduction and thus should not be considered. Both concentrations of 1.56 w% and 2.61 w% resulted in a large decrease of drying shrinkage and both show consistent predictable influences on the hydration process and mechanical properties. However, increasing the concentration from 1.56 w% to 2.61 w% has diminishing returns on the shrinkage reduction and negatively influences the other properties. It is also more expensive. Therefore, the user should consider if the added drying shrinkage reduction of 2.61 w% SRA is worth the added costs and further reduction of mechanical properties with respect to lower SRA concentrations.

As this research was conducted in an experiment environment with relatively small samples, for the construction work field it would be interesting and recommended to conduct some field experiments. Hereby, the use of concrete mixtures with the applied SRA could give insight into the long-term effects of the SRA on concrete. In addition, more experimenting is necessary to gain valuable information for upscaling to practice. For example, experimenting with samples where reinforcement is applied to test restrained shrinkage behavior can be valuable. Trying out different water to cement ratios and adding different additives could be interesting to limit some less preferred effects of the SRA.

6.2) Scientific implications & recommendations

Within the field of concrete science less was known about the mechanism of shrinkage reduction and influences of SRAs on the hydration process and on the material properties of concrete. This research was a first step to investigate this by looking at the influences of the SRA Sika Control 40. All in all, the results have shown that drying shrinkage is reduced by the SRA. However, this also has its implications for the other properties of concrete.

A specific set of experiments have been chosen in the set up for this research. These experiments were chosen to obtain a general overview on the mechanism of shrinkage reduction and influences of applying Sika Control 40 in concrete. To expand on this research, influences of SRA on creep, relaxation and restrained deformation could be investigated. Because these play an important role on shrinkage strains and crack formation. Also, the effect of changing the water to cement ratio with fixed SRA content can be a topic for future research. Changing the water to cement ratio influences the hydration rate and strength development of concrete. This test could result in an optimal water to cement ratio where the SRA performs best. From test results a decrease in rate of hydration was observed. In section 4.1.2 Isothermal calorimetry (hydration rate) an exploration of possible causes was added. Because this phenomenon could not be fully explained here, future research could investigate that to further extent.

Altogether, this research has given an interesting view on both the practical and scientific implications of using the SRA Sika Control 40 in concrete. The information obtained on Sika Control 40 can result in more durable concrete structures, while achieving a reduction in the usage of building materials.

References

Aldridge, B. & Brar, N. (2019, October 22). *Surface Tension.* https://chem.libretexts.org/Bookshelves/Physical_and_Theoretical_Chemistry_Textbook_Maps/Supplemental_Modules_(Physical_and_Theoretical_Chemistry)/Physical_Properties_of_Matter/States_of_Matter/Properties_of_Liquids/Surface_Tension

Andrew, R. M. (2018). Global CO 2 emissions from cement production, 1928–2017. *Earth System Science Data*, *10*(4), 2213-2239.

Anstice, D. J., Page, C. L., & Page, M. M. (2005). The pore solution phase of carbonated cement pastes. *Cement and Concrete Research*, *35*(2), 377-383.

Ben Mya, O. (2020). Easy way to understand SURFACE PHENOMENA and SOLID CATALYSTS A Polycopie addressed to students of Process Engineering & Petro chemistry. 10.13140/RG.2.2.34889.70241.

Bentz, D. P., Peltz, M. A., & Winpigler, J. (2009). Early-age properties of cement-based materials. II: Influence of water-to-cement ratio. *Journal of materials in civil engineering*, *21*(9), 512-517.

Carballosa, P., Calvo, J. G., Revuelta, D., Sánchez, J. J., & Gutiérrez, J. P. (2015). Influence of cement and expansive additive types in the performance of self-stressing and self-compacting concretes for structural elements. *Construction and Building Materials*, *93*, 223-229.

Chemistry Libretexts. (2019, June 5). *Chapter 6.3: VSEPR - Molecular Geometry.* https://chem.libretexts.org/Courses/Howard_University/General_Chemistry%3A_An_Atoms_First_Approach/Unit_2%3A__Molecular_Structure/Chapter_6%3A_Molecular_Geometry/Chapter_6.3%3A_VSEPR_-_Molecular_Geometry

Collepardi, M., Borsoi, A., Collepardi, S., Olagot, J. J. O., & Troli, R. (2005). Effects of shrinkage reducing admixture in shrinkage compensating concrete under non-wet curing conditions. *Cement and Concrete Composites*, *27*(6), 704-708.

Craeye, B., Geirnaert, M., & De Schutter, G. (2011). Super absorbing polymers as an internal curing agent for mitigation of early-age cracking of high-performance concrete bridge decks. *Construction and building materials*, *25*(1), 1-13.

Eberhardt, A. B. (2010). On the mechanisms of shrinkage reducing admixtures in self con-solidating mortars and concretes.

Grădinaru, Cătălina. (2017). The Environmental Impact of Concrete Production and the Necessity of its Greening.

Jensen, O. M., & Bentz, G. (2002). On the mitigation of early age cracking. In *On the Mitigation of Early Age Cracking* (pp. 195-203).

Jensen, O. M., & Lura, P. (2006). Techniques and materials for internal water curing of concrete. *Materials and Structures*, *39*(9), 817-825.

Hind, M. K., Özakça, M., & Ekmekyapar, T. (2016). A review on nonlinear finite element analysis of reinforced concrete beams retrofitted with fiber reinforced polymers. *Journal of Advanced Research in Applied Mechanics*, *22*(1), 13-48.

Li, J., & Yao, Y. (2001). A study on creep and drying shrinkage of high performance concrete. *Cement and Concrete Research*, *31*(8), 1203-1206.

Lura, P. (2003). Autogenous deformation and internal curing of concrete.

Maltese, C., Pistolesi, C., Lolli, A., Bravo, A., Cerulli, T., & Salvioni, D. (2005). Combined effect of expansive and shrinkage reducing admixtures to obtain stable and durable mortars. *Cement and concrete research*, *35*(12), 2244-2251.

Mather, B. (1970). *Expansive cements* (Report No. C-70-2). Wicksburg, Mississippi: U. S. Army Engineer Waterways Experiment Station.

Morini, M. A., Messina, P. V., & Schulz, P. C. (2005). The interaction of electrolytes with non-ionic surfactant micelles. *Colloid and Polymer Science*, *283*(11), 1206-1218.

Nagataki, S., & Gomi, H. (1998). Expansive admixtures (mainly ettringite). *Cement and concrete composites*, *20*(2-3), 163-170.

Neville, A. (1995). *Properties of concrete* (4th edition). Essex, England: Longman Group Limited.

Particle Technology Labs. (n.d.). *Mercury Intrusion Porosimetry.* https://www.particletechlabs.com/analytical-testing/gas-adsorption-and-porosimetry/mercury-intrusion-porosimetry

Rajabipour, F., Sant, G., & Weiss, J. (2008). Interactions between shrinkage reducing admixtures (SRA) and cement paste's pore solution. *Cement and Concrete Research*, *38*(5), 606-615.

Reinhardt, H. W. (1998). *Beton als constructiemateriaal: eigenschappen en duurzaamheid*. Delft, Nederland: Delftse Universitaire Pers.

Rosen, M. J. (2004). *Surfactants and Interfacial Phenomena* (3rd ed.). Hoboken, New Jersey: John Wiley & Sons, Inc..

Sant, G. (2012). The influence of temperature on autogenous volume changes in cementitious materials containing shrinkage reducing admixtures. *Cement and concrete composites*, *34*(7), 855-865.

Shah, S. P., Krguller, M. E., & Sarigaphuti, M. (1992). Effects of shrinkage-reducing admixtures on restrained shrinkage cracking of concrete. *Materials Journal*, *89*(3), 289-295.

Sika Group. (2014, October 10). *Sika Control-40 Shrinkage Reducing Admixture.* https://usa.sika.com/content/dam/dms/us01/1/pds-cpd-Sika%20Control%2040-us.pdf

Szilágyi, K., Zsigovics, I., & Szautner, C. (2007). Advanced shrinkage compensation of concretes by a combined admixture system. *Építőanyag*, *59*.

Wadso, L. (1995). The study of cement hydration by isothermal calorimetry. *Building Materials, Lund University, Sweden*.

Winnefeld, F., & Lothenbach, B. (2010). Hydration of calcium sulfoaluminate cements—experimental findings and thermodynamic modelling. *Cement and Concrete Research*, *40*(8), 1239-1247.

Zhan, P. M., & He, Z. H. (2019). Application of shrinkage reducing admixture in concrete: A review. *Construction and Building Materials*, *201*, 676-690.

Zhang, T., Gao, P., Luo, R., Guo, Y., Wei, J., & Yu, Q. (2013). Measurement of chemical shrinkage of cement paste: Comparison studyof ASTM C 1608 and an improved method.

Zuo, W., Feng, P., Zhong, P., Tian, Q., Gao, N., Wang, Y., ... & Miao, C. (2017). Effects of novel polymer-type shrinkage-reducing admixture on early age autogenous deformation of cement pastes. *Cement and Concrete Research*, *100*, 413-422.

Appendix A: Surfactants

In this appendix more in depth information can be found on surfactants. Extra information can be found on the chemical composition and on its behaviour.

Shrinkage reducing agents

Shrinkage reducing agents (SRAs) are a type of surfactant. It is a chemical with a hydrophilic and a hydrophobic part that can lower the surface tension. The surfactant will place itself on the boundary of water with concrete oriented with the hydrophilic part towards the water and the hydrophobic part towards the concrete (Rosen, 2004). This occurs because the total free energy of the solution will be lowered, there is less entropy in the system, and this is energetically more favourable. To get a better understanding in the way shrinkage reducing agents work we will first take a closer look at surface tension and capillary action. Then a closer look is taken into surfactants and their mechanisms.

Surfactants

As said before most of the shrinkage reducing agents are surfactants. Surfactants can be detergents, foaming agents, wetting agents, emulsifier, and dispersants. These different surfactant types have different chemical compositions. They can even work differently to reduce surface tension. This all has to do with the hydrophobic and hydrophilic groups these surfactants have. The hydrophobic part of the surfactant molecule is the part that does not want to bond with water molecules. The hydrophilic part wants to bond with the water molecules. As stated earlier, there are different kinds of hydrophobic and hydrophilic parts (Rosen, 2004). An overview of different hydrophobic groups is shown below, and some influences are explained.

1. Straight-chain, long alkyl groups (C_8–C_{20})
2. Branched-chain, long alkyl groups (C_8–C_{20})
3. Long-chain (C_8–C_{15}) alkylbenzene residues
4. Alkylnaphthalene residues (C_3 and greater-length alkyl groups)
5. Rosin derivatives
6. High-molecular-weight propylene oxide polymers (polyoxypropylene glycol derivatives)
7. Long-chain perfluoroalkyl groups
8. Polysiloxane groups
9. Lignin derivatives

Figure 2.5 Hydrophobic groups (Rosen, 2004)

Length of hydrophobic group: Longer chains means; less soluble in organic solvents; closer packing of surfactant at interface; increases tendency to form micelles; increases melting point; increases sensitivity. To increase solubility, you would like a short hydrophobic group, but that also means that the packing is less favourable. When the packing is less favourable there will be less molecules at the interface. The surfactant molecules will be in the bulk solution earlier when the hydrophobic chain is longer. Therefore, longer chains will form micelles at lower concentrations with the result that the critical concentration of the surfactant will be lower. A balance should be found for the length of the hydrophobic chain.

Branching, unsaturation: branching and unsaturation; increases solubility; decreases melting point; causes looser packing of surfactant at interface; may cause oxidation and colour formation in unsaturated compound; decreases biodegradability; increases thermal instability. The same problem occurs for branching as for the length of the hydrophobic chain. Branching increases solubility but it decreases the critical concentration of the surfactant. A balance should be found for the number of branches as well.

Aromatic nucleus: The presence of an aromatic nucleus; increases adsorption of surfactant on polar interfaces; decreases biodegradability; causes looser packing of surfactant at interface.

Polyoxypropylene or polyoxyethylene units: polyoxypropelene increases hydrophobic nature, increases adsorption onto polar surfaces and solubility in organic solvents. Polyoxyethylene decreases hydrophobic character.

Perfluoroaklyl or polysiloxane group: These groups have a positive result on the minimal achievable surface tension of water when compared to hydrocarbon based hydrophobic groups.

As shown above surfactants can have very different molecular compositions. Nevertheless, they have one thing in common: they all have a hydrophilic and a hydrophobic part. The hydrophilic part can be anodic, cathodic, non-ionic and zwitterionics. Anodic surfactants have a negative charge at the surface-active part, for example RCOO-Na+. Cationic surfactants bear a positive charge at the surface-active part, RNH_3+Cl-. Non-ionic surfactants bear no charge at the surface-active part. Zwitterionic surfactants bear both positive and negative charges. These four different types interact in different ways with the cement and the capillary pore water. Which also lowers the surface tension by different amounts. Hydrocarbon surfactants can reduce the surface tension down to about 30mN/m and fluorocarbon surfactants to about 20mN/m.

Sika Control 40

As this research is based on the Sika Control 40 admixture, we take a closer look at its functionality. Sika control 40 consists of neopentyl glycol, this is a double alcohol molecule. This makes it a non-ionic surfactant. Rosen (2004) states the advantages and disadvantages of polyolefin elastomers straight chain alcohols (alcohol ethoxylates, AE) which is like the neopentyl glycol in behaviour. The first advantage is that the structure of the AE can be optimized for performance since the average hydrophobic, hydrophile and distribution of the ethoxymers can be varied. In addition, AES are more tolerant of high ionic strength and hard water and they are more stable in hot alkaline solutions. These characteristics are especially beneficial when applied in cement. Cement has a lot of ionic bonding and the pore water solution contains a lot of calcium carbonate, so it is 'hard water'. During hydration the concrete will heat up so there will be a hot alkaline environment where this surfactant has an optimal performance. One of the disadvantages is that in high concentrations AES tends to bleed from powders giving poor powder properties. Besides, AES can impart an objectionable odour to the ethoxylate in high concentrations. Since, Sika control 40 is applied in liquid form and the applied concentrations are relatively low, the odour might not be a problem. Given the pros and cons, Sika control 40 looks like a surfactant that can work like it is supposed to.

To research the behaviour and mechanics of Sika Control 40 the bonding behaviour is investigated. As stated previously the different surfactant types will work in different ways (Rosen, 2004). Anionic and cathodic surfactants will use ion exchange and ion-pairing at the water-concrete interface. Ion exchange involves the replacement of counter ions absorbed onto the solid substrate by similarly charged surfactant ions, so this is dependent on diffusion rate. Ion pairing is the adsorption of surfactant ions from solution onto oppositely charged sites unoccupied by counter ions. Non-ionic surfactants like the Sika control 40 work via hydrogen bonding or via Lewis acid-Lewis base reaction. These mechanisms are shown below.

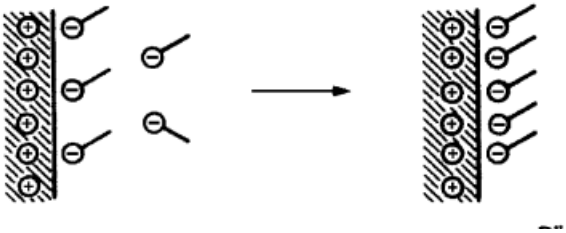

Figure 2.6 Ion pairing (Rosen, 2004)

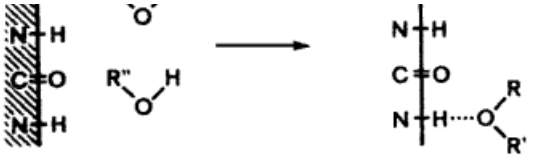

Figure 2.7 Hydrogen bonding (Rosen, 2004)

So, the Sika Control 40 molecules take the place of the water molecules at the interface between the water and concrete. This way the forces that will be induced by the surface tension of the water will be lowered resulting in lower capillary tensile stresses and ultimately in less drying shrinkage.

In figure 2.8 the shrinkage reduction in SRA modified mortars dependant of dosage and time is shown (Eberhardt, 2010). Table 1 shows the exact values. The major part of shrinkage reduction is gained in the first 50 days well before drying equilibrium is reached. After approximately 30 days of drying the absolute increase in shrinkage proceeds independently of the SRA dosage (Eberhardt, 2010).

time	shrinkage reduction [%]		
14d	37	44	57
28d	17	26	39
70d	16	20	32
180d	12	14	28
364d	10	14	24
SRA*	1.5%	2.5%	5.0%

*wt.-% of mixing water

Table 2.0.1 Free drying shrinkage of SRA mixes with different concentrations as a function of time (Eberhardt, 2010)

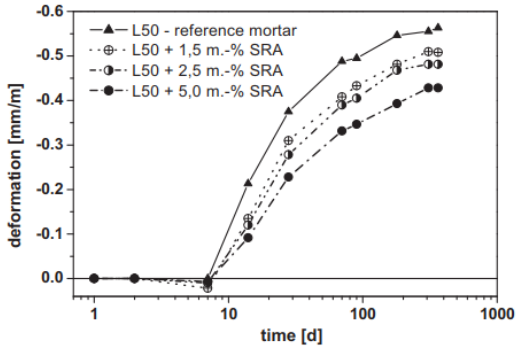

Figure 2.8 Free drying shrinkage of SRA mixes with different concentrations as a function of time (Eberhardt, 2010)

Collepardi et al. (2005) researched the amount of shrinkage reduction of concrete with SRA based on neopentyl glycol, like Sika control 40. In concrete with a w/c ratio of 0.40, 390 kg/m^3 cement content and 1 week of wet curing it can be observed in figure 2.10 that the shrinkage reduction is approximately 35-40% when the concrete is exposed to 25 degrees Celsius air temperature and 60% relative humidity.

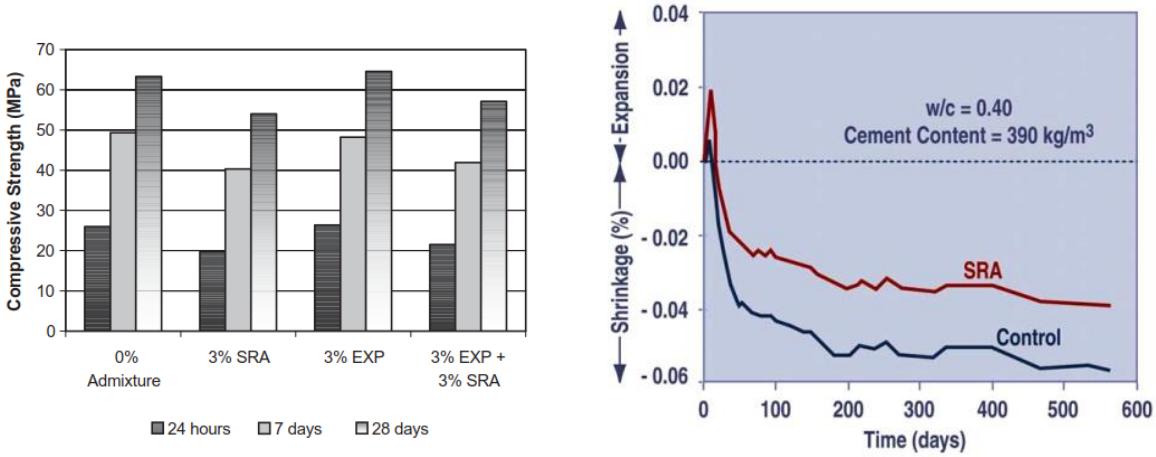

Figure 0.1 Shrinkage reductions with SRA similar to Sika Control 40. 390 kg/m³ cement, 0.4 w/c and one week wet curing at 25 degrees Celsius. (Collepardi et al., 2005)

Downsides of applying SRA

SRA can have a multitude of influences on the hydration process and therefore, the mechanical properties of concrete. Even different concentrations of SRA can result in different behaviour. To understand these mechanisms and their influences, downsides of applying SRA are discussed below.

Possible loss of surfactant at the solid liquid interface: For Sika Control 40 to work it must be in the pore solution. If the SRA is absorbed or aggregates on the cement surface it loses effectivity. The hydrated cementitious environment has a high concentration of electrolyte. The shrinkage reducing agent in the pore solution is exposed to these electrolytes. The hydration product also has a very high internal specific area, especially low-density calcium hydroxide. The large number of electrolytes and the large specific area can enhance the absorption/aggregation of surfactant at the solid liquid interface as well as a salting out effect. Salting-out is a reduction in solubility of SRA in the pore solution. This mechanism is ion driven.

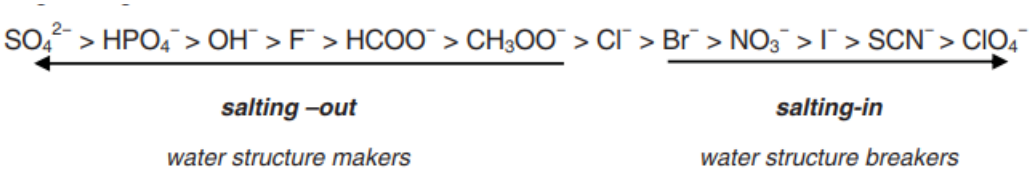

Figure 2.10.2 Salting-in and salting-out ions (Rosen MJ, 2004

Ions left of Cl^- are called cosmotropic or water structure makers. They reduce the solubility of protein in water. These ions reduce the chaos in the water structure. The water molecules are arranged more organized around these ions so that the surfactant molecules have less possibilities to hydrogen bond. Thus, lowering the solubility of surfactants in the water. The ions right of Cl^- are called water structure breakers and they increase the solubility of water because the water molecules are ordered more chaotic around these ions thus making it easier to hydrogen bond with the surfactant. The figure only shows the anions, but cations can also cause salting-in and salting-out effects (Morini, Messina, & Schulz, 2005). In cementitious materials you have Ca^{2+} and Al^{3+} ions according to Morini et al. this implies that salting-in may occur. Bowton & Finney showed that non-ionic surfactants in cementitious environment are also subjected to salting-out. This has to do with the fact that due to direct anion-bridging the alcohol reorganises so that four polar groups point towards the polar group of a central alcohol molecule. So, both salting-in and slating-out can occur therefore the question arises which one will be dominant. Rosen 2004 investigated the influence of ions on the critical micelle concentration

(CMC) in aqueous electrolyte solutions of non-ionic surfactants. He found the following influence on salting-out for anions:

$$SO_4^{2-} > F^- > BrO_3^- > Cl^- > Br^- > NO_3^- > I^- > SCN^-$$

And for cations:

$$NH_4^+ > K^+ > Na^+ > Li^+ > {}^1/_2\, Ca^{2+}$$

Due to the nature of the cementitious materials there will be a lot of alkaline ions in the pore solutions like Na^+, K^+ and $1/2Ca^{2+}$. This will enhance the salting-out of non-ionic surfactants which may affect the possible shrinkage reduction because the surfactants might self-aggregate by forming micelles lowering the critical micelle concentration. A lower critical micelle concentration results in a higher minimal surface tension.

Adsorption of the surfactant onto the solid/liquid interface: Due to the amphiphilic nature of non-ionic surfactants they can adsorb on both hydrophilic and hydrophobic surfaces. Bonding onto hydrophilic surfaces will be due to hydrogen bonding of the polar parts with silanol, silica and amorphous quartz, and/or aluminol groups like clay. The adsorption will decrease drastically at higher pH values. These groups will be deprotonated at higher pH values. Either the dissolution of these minerals or the strong increase in surface charge is expected to be responsible for this decreased adsorption. At low concentrations it is possible for non-ionic monomers to be adsorbed onto the solid surface. More interactions like these will occur with higher surfactant concentrations. The surface coverage will increase. At the critical aggregation concentration, CAC, the adsorption will increase because there will be micelle aggregation at the surface of the solid. The CAC is a specific bulk concentration of the surfactant. Due to this aggregation at the solid/liquid interface you will lose a fraction of surfactant that can actively decrease the surface tension. The adsorption at the solid/liquid interface will increase at higher temperatures. Higher temperatures increase solubility which increases the adsorption at the solid/liquid interface because higher temperature increase the water breaking behaviour of salting-out ions. The surfactant will self-aggregate easier with the monomers at the solid interface.

Appendix B: Typical Low shrinkage concrete mix design

Typical low shrinkage cement used for concrete floor slabs in the Netherlands (ABT bv, 2019):

Zeven volgens NEN 2560	Rivierzand 0/4	Riviergrind 4/32	Riviergrind 4/16	Mengsel
Toeleveringscode	15751	15752	15753	
C 63 mm	0,0%	0,0%	0,0%	0,0%
C 45 mm	0,0%	0,0%	0,0%	0,0%
C 31.5 mm	0,0%	1,0%	0,0%	0,4%
C 22.4 mm	0,0%	16,0%	0,0%	6,8%
C 16 mm	0,0%	41,0%	0,0%	17,5%
C 11.2 mm	0,0%	62,0%	22,4%	29,7%
C 8 mm	0,0%	77,0%	51,0%	40,2%
C 5.6 mm	0,0%	88,0%	76,5%	48,5%
C 4 mm	5,0%	95,0%	91,8%	55,8%
C 2 mm	16,0%	99,0%	99,0%	63,3%
1 mm	30,0%	100,0%	100,0%	69,9%
500 µm	60,0%	100,0%	100,0%	82,8%
250 µm	91,0%	100,0%	100,0%	96,1%
125 µm	98,0%	100,0%	100,0%	99,1%
63 µm	100,0%	100,0%	100,0%	100,0%
Rest	100,0%	100,0%	100,0%	100,0%
Fijnheidmodulus	3,00	7,13	6,42	5,25
Vocht	0,5%	1,6%	1,6%	
Absorptie	0,5%	1,6%	1,6%	
Verhouding toeslag	100,00%	74,85%	25,15%	
Fractie	43,00%	42,67%	14,33%	
Vol. massa	2,60kg/L	2,58kg/L	2,56kg/L	

Sterkte klasse	LOS
Statistische milieu klasse	(-)
Milieuklasse	(-)
Milieuklasse	X0-Geen corrosie of aantasting
Consistentie	Schudmaatklasse F4
Maximale korrelgrootte	DMax = 32
Wapening	Gewapend
Chloride klasse	Cl 0,40
wbf / wcf	0,500 / 0,509
Zand (t.o.v. toeslag)	43,00% V/V
Chloridegehalte (tot bindmiddel)	0,06% M/M
Alkaligehalte	2,49kg
Luchtgehalte	18,0L
Temperatuur:	12°C
waterbehoefte	171,1L
Aanmaakwater	174,5L
Eff. aanmaakwater (zonder slib)	171,1L
Geabsorbeerd water	19,8L
Aanhangend vocht	19,8L

Grondstoffen	producent	Te doseren massa	Droge massa	Volume fijn	T.o.v. cement
CEM III/B 42,5 N Maastricht	Enci Maastricht	336kg	336kg	114,0L	
Rivierzand 0/4	Teunesen	764kg	760kg	26,3L	
Riviergrind 4/32	Merwede 28	760kg	748kg	0,0L	
Riviergrind 4/16	Merwede 28	253kg	249kg	0,0L	
Poederkoolvliegas (met K-factor)	Euroment	30kg	30kg	13,0L	
CUGLA LR9700 con 30%	Cugla	1,042kg	1,042kg	0,0L	0,31% m/m
Slibwater	Voorraad	106kg	106kg	3,4L	
Bronwater	Voorraad	73kg	73kg	0,0L	
Lucht		18L	18L	0,0L	
Totaal		**2324kg**		**156,7L**	

Appendix C: Concrete mix design for experiments

Concrete mix design for concrete samples (ABT bv, 2019). The amount of SRA is subtracted from the added mixing water.

Uitlevering

Naar berekening benodigd volume | Naar INHOUD

Gehalte fijn is 144 liter/m^3			Uitlevering per 1 m³ (bij droog toeslagm.) kg	liter	Af te wegen in **kg** voor gewenste mengselgrootte (bij nat toesl.mat.): voor 1m³	100 liter beton	volume nat voor 100 liter	Kosten per 1 m³ in euro's
CEM III/B 42,5 N LH/HS Cemij	CEM III/B 42,5 N LH/HS Cemij		350,0	118,64	350,00	**35,00** kg	11,86	31,50
geen cement	geen tweede cement		0,0	0,00	0,00	**0,00** kg	0,00	0,00
Toe te voegen aanmaakwater: Leidingwater			147,8	147,789	147,789	**14,779** kg	14,779	0,443
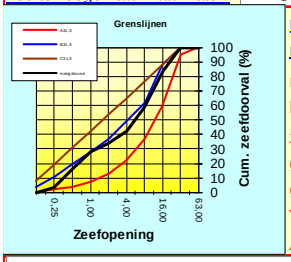	riverzand 0/4	40%	735,0	277,34	738,63	**73,863** kg	27,73	7,35
	riviergrind 4/3	40%	735,0	277,34	757,01	**75,701** kg	43,90	5,00
	riviergrind 4/1	20%	367,5	138,67	374,46	**37,446** kg	17,91	7,35
	liapor 0-4	0%	0,0	0,00	0,00	**0,000** kg	0,00	0,00
	z 2-4mm	0%	0,0	0,00	0,00	**0,000** kg	0,00	0,00
	g 4 -8mm	0%	0,0	0,00	0,00	**0,000** kg	0,00	0,00
	g 8 -16mm	0%	0,0	0,00	0,00	**0,000** kg	0,00	0,00
	VAR 4-16	0%	0,0	0,00	0,00	**0,000** kg	0,00	0,00
	AEB 6-20	0%	0,0	0,00	0,00	**0,000** kg	0,00	0,00
geen puzzolane vulstof 1	k-waarde:	1,00	0,0	0,0	0,0	**0,000** kg	0,0	0,00
geen vulstof 2		n.v.t.	0,0	0,0	0,0	**0,000** kg	0,0	0,00
geen vulstof 3		n.v.t.	0,0	0,0	0,0	**0,000** kg	0,0	0,00
vezeltype 1	geen vezels		0	0,0	0,0	**0,000** kg	0,0	0,00
vezeltype 2	geen vezels		0	0,0	0,0	**0,000** kg	0,0	0,00
luchtbelvormer	geen luchtbelvormer	0%	0,000	0,000	0,000	**0,000** kg	0,000	0,00
superplastificeerder	geen superplastificeerder	0%	0,000	0,000	0,000	**0,000** kg	0,000	0,00
versneller	geen versnellers	0%	0,000	0,000	0,000	**0,000** kg	0,000	0,00
vertrager	geen vertragers	0%	0,000	0,000	0,000	**0,000** kg	0,000	0,00
andere hulpstof	geen extra hulpstof	0%	0,000	0,000	0,000	**0,000** kg	0,000	0,00
ingesloten lucht 2 %		2%	0	20	0		2,0	**Totaal**
Het chloride gehalte is 0,1 % en is voldoende laag								**51,64**

Vrijkomend water uit luchtbelvormer:			0,0	0,0				w/c	0,480
Vrijkomend water uit superplastificeerder:			0,0	0,0				w/(c+k.v)	0,480
Vrijkomend water uit overige hulpstoffen:			0,0	0,0				(w+l)/(c+k.v)	0,480
water uit puzzolanen:			0,0	0,0				c (kg/m³)	350
water uit vulstof 2:			0,0	0,0				c+k.v	350
water uit vulstof 3:			0,0	0,0					
Aanhangend water aan de toeslagkorrels: dus vrij komend water:			20,2	20,2					
Geabsorbeerd water in de toeslagkorrels, dus niet vrij komend water:			12,5	0,0				Dnom 31,5 mm	
Pas op, U haalt de gewenste betonkwaliteit C45 niet!								De mengselcurve voldoet	
Totaal vrij water:			168	168,0				wel aan de lijn A32-C32	
				0,0				wel aan de lijn A32-B32	
Totale massa (kg):			2368		2368	236,79	kg		
Totaal volume (liter):				1000		118	liter beton		

Naam:	Mengselprogramma dr.ir. A. Fraaij	Milieuklasse	X0: Geen risico voor aantasting, beto	Betonkwaliteit	C35/45
Omschrijving mengsel:		Oppervlaktebehandeling	geen oppervlakte nabewerking		
Datum	8 mei 2008	Soort wapening	gewapend beton		
Studienummer:	Versie 39	Consistentiegebied	vloeibaar	met gemiddelde zetmaat 220 mm	
Opmerkingen over het mengsel:		Elementtype	wand	Soort beton	normaal beton
Omschrijving toeslagmateriaal:	Rivierzand en -grind en menggranu	Gebruiksdoel	pompbeton		
Naam toeslagfractie 1:	riverzand 0/4	Betondekking (mm)	76	Pastalaagdikte rond z+g (micron)	79,66
Naam toeslagfractie 2:	riviergrind 4/32			Waterlaagdikte rond <125 mu (micron)	1,04

Voor opgave porositeit korrels: ga naar porositeitkorrels

Voor opgave vrij en gebonden water aan en in de korrels: ga naar vochtgehalte

Voor volumieke massa toeslagmateriaal: ga naar volumiekemassa

U moet een superplastificeerder toepassen